Geothermometry of Thermal Springs
in the
Rico, Dunton, and West Fork Dolores River Areas, Dolores County, Colorado

By
Erik J. Oerter

John W. Hickenlooper, Governor
State of Colorado

Mike King, Executive Director
Department of Natural Resources

Vincent Matthews
State Geologist and Director
Colorado Geological Survey

Colorado Geological Survey
Department of Natural Resources
Denver, Colorado
2011

FOREWORD

This report describes the location, physical setting, hydrochemistry, and geothermometry of ten thermal springs or wells in the Rico Group and West Fork Group of the Dolores River areas of Colorado. Geothermometry is a technique used to estimate the subsurface temperature of a geothermal reservoir, or the most recent temperature at which the water has undergone chemical reactions. This information is useful in geothermal exploration when considering the resource potential of an area. Statewide, Colorado has a significant geothermal power generation potential, and the area centered on the Town of Rico is among the highest heat flow areas in the State.

Recently, there has been increased interest in renewable sources of energy because of the increasing costs of fossil fuels and environmental impacts from the use of fossil fuels. Geothermal energy is a renewable form of energy that at higher temperatures (circa 150°C/300°F or more) can be used for producing electrical power and at somewhat lower temperatures can be used directly for heating of buildings, industrial processes, greenhouse agriculture, aquaculture, and recreational/health resorts. This report provides important information to help determine the temperature and potential uses of the geothermal resources near Rico and Dunton.

This project was jointly funded by the Governor's Energy Office[1] and the Colorado Geological Survey (Colorado Department of Natural Resources Severance Tax Operational Fund). Severance taxes are derived from the production of gas, oil, coal, and minerals.

Matthew A. Sares
Deputy Director

Vincent Matthews
State Geologist and Division Director

---

[1] Support by the Governor's Energy Office does not constitute their endorsement of the views expressed in this report.

CONTENTS

FIGURES

Tables

LIST OF ABBREVIATIONS AND SYMBOLS

C	Celsius or centigrade
CGS	Colorado Geological Survey
cm	centimeter(s)
gpm	gallons per minute
HDPE	High Density Polyethylene
km	kilometer
LMWL	Local Meteoric Water Line
mL	milliliter
mg/L	milligrams per liter
mS	milliSiemens
mW/m^2	milliwatts per square meter
n/a	not applicable
NEG	negative value
NM	not measured
p.	page(s)
ppm	parts per million
T	temperature
U.S.	United States
USFS	United States Department of Agriculture - Forest Service
USGS	United States Geological Survey
v	Volume
VSMOW	Vienna Standard Mean Oceanic Water
~	approximate value
°	degree
>	greater than
<	less than
≤	less than or equal to
µg/L	micrograms per liter
µ	microns
µS/cm	microSiemens per centimeter
#	number
%	percent
‰	per mil
δ	delta
‘	feet
“	inches

1. Introduction

Recent work by the Colorado Geological Survey assessed the statewide distribution of heat flow (Berkman and Carroll, 2007) and geothermal gradient (Berkman and Watterson, 2010) in Colorado. Maps produced by this work indicate an area of high heat flow and high geothermal gradient centered on the Town of Rico in southwest Colorado (Figures 1 and 2). In the Rico area several hot springs and wells are surface expressions of geothermal heat at some depth. These recent heat flow and gradient data indicate a geothermal resource with potential for direct use in recreational spas and pools, agriculture, greenhouses, light industrial processes, and space heating situations. In addition, potential may exist for producing electricity. On the other hand, data from previous studies (Barrett and Pearl, 1978) indicate, through geothermometry, that the temperature at depth is not much more than that expressed at the surface. The purpose of this study was to investigate improvements in geothermometry methods to determine if better control and confidence could be attained regarding geothermal resource temperatures at depth.

Geothermometry is the use of chemical constituent concentration data from geothermally heated waters to infer the temperature at which those waters evolved. More accurately, geothermometry estimates the last temperature at which the water underwent various chemical reactions with the surrounding rock.

Immediately north of the Town of Rico is a group of three springs and four flowing drill holes that comprise the Rico Group (Figure 3). Along the West Fork of the Dolores River and its tributary Geyser Creek are three springs that comprise the West Fork of the Dolores Group. Some of these springs and drill holes were previously sampled in 1975 and 1976 and re-sampled in July of 2008. These various data sets are combined, analyzed, and discussed in this report.

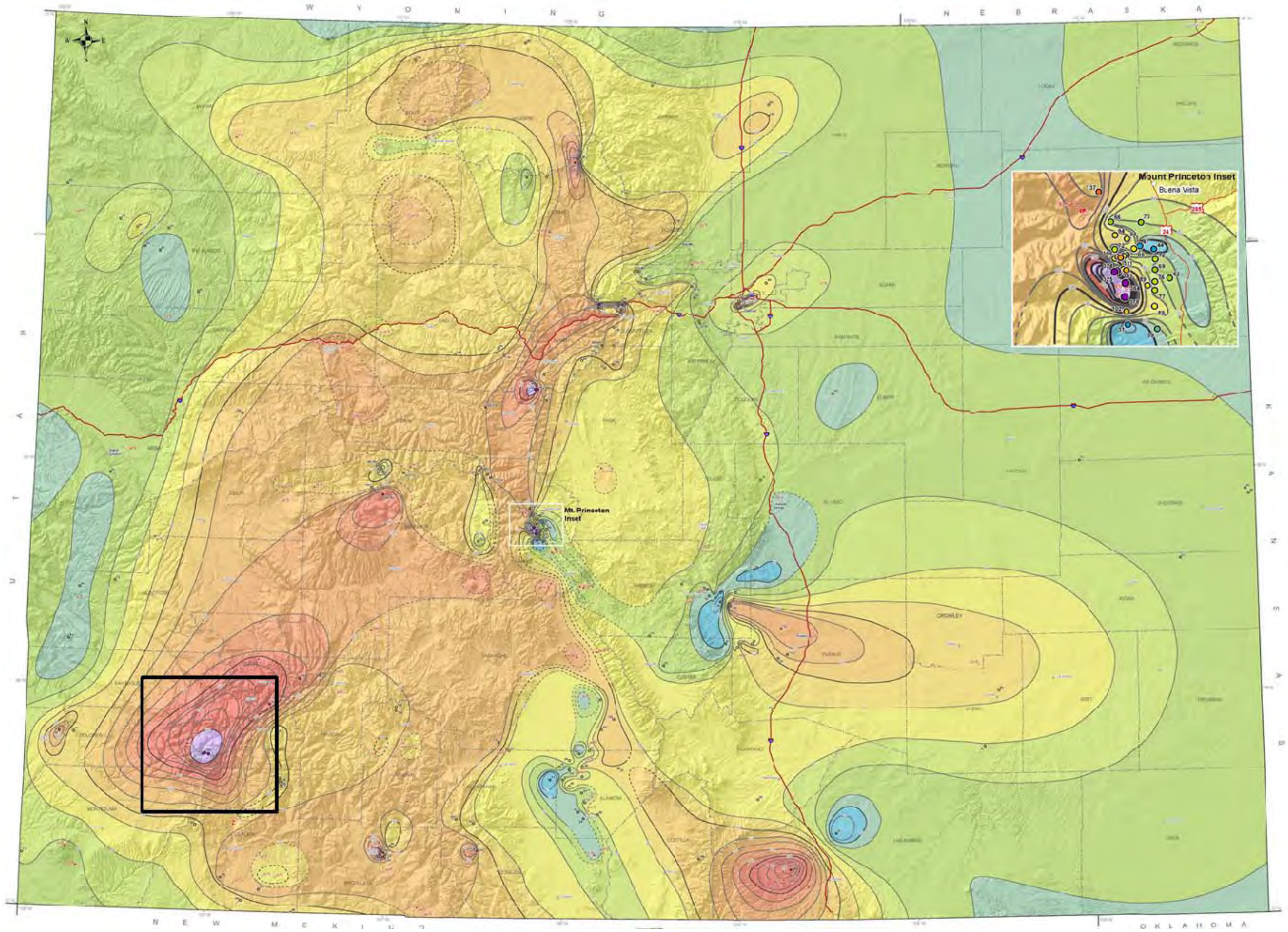

Figure 1. Map of heat flow in Colorado. Areas of higher heat flow are indicated by warmer colors, with purple being warmest (units are mW/m^2). Study area is in the black box in the lower left corner of map (Berkman and Carroll, 2007).

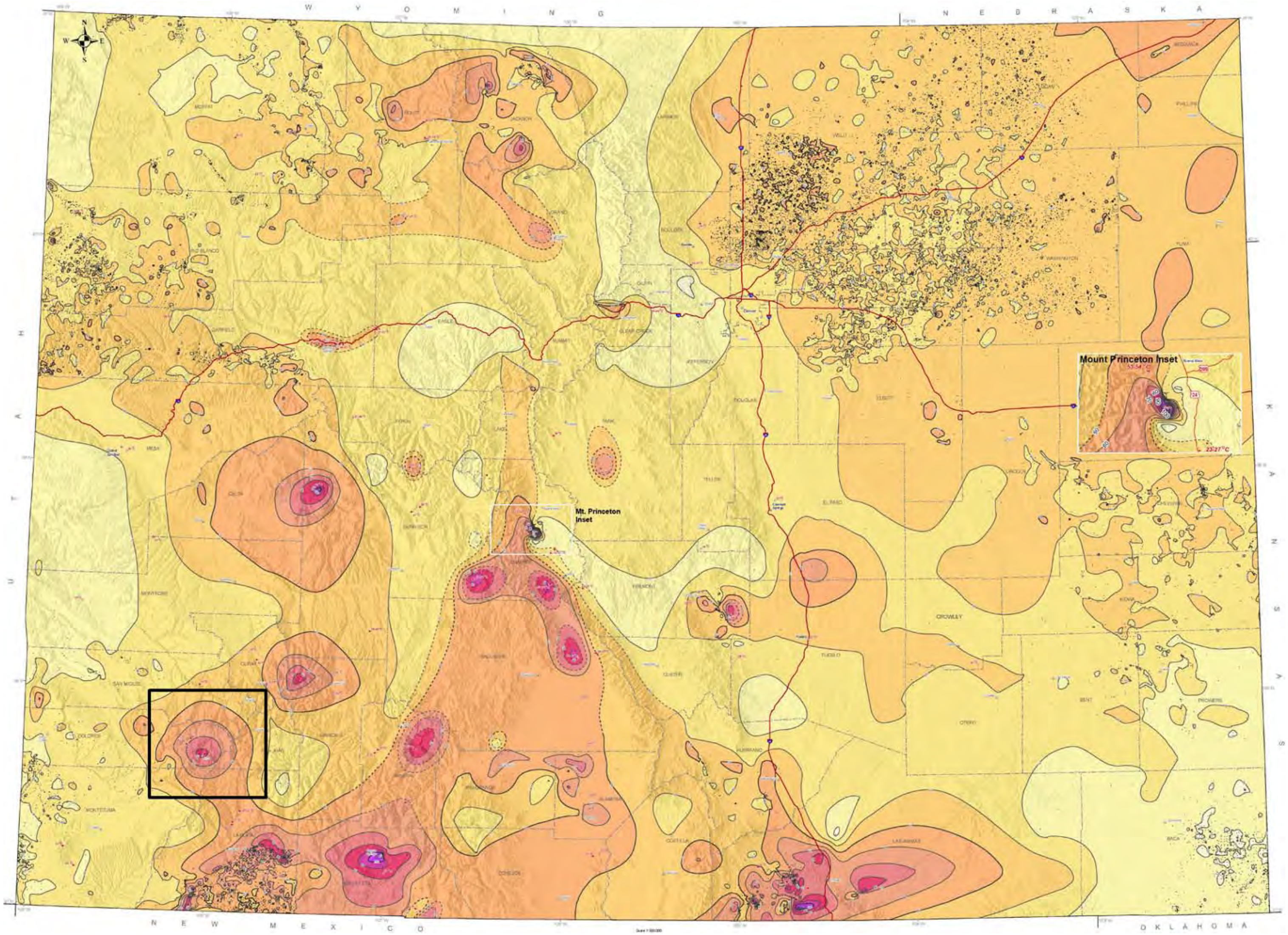

Figure 2. Geothermal gradient map of Colorado. Areas of higher geothermal gradient are indicated by warmer colors, with red being highest (units are ºC/km). Study area is in the black box in the lower left corner of map (Berkman and Watterson, 2010).

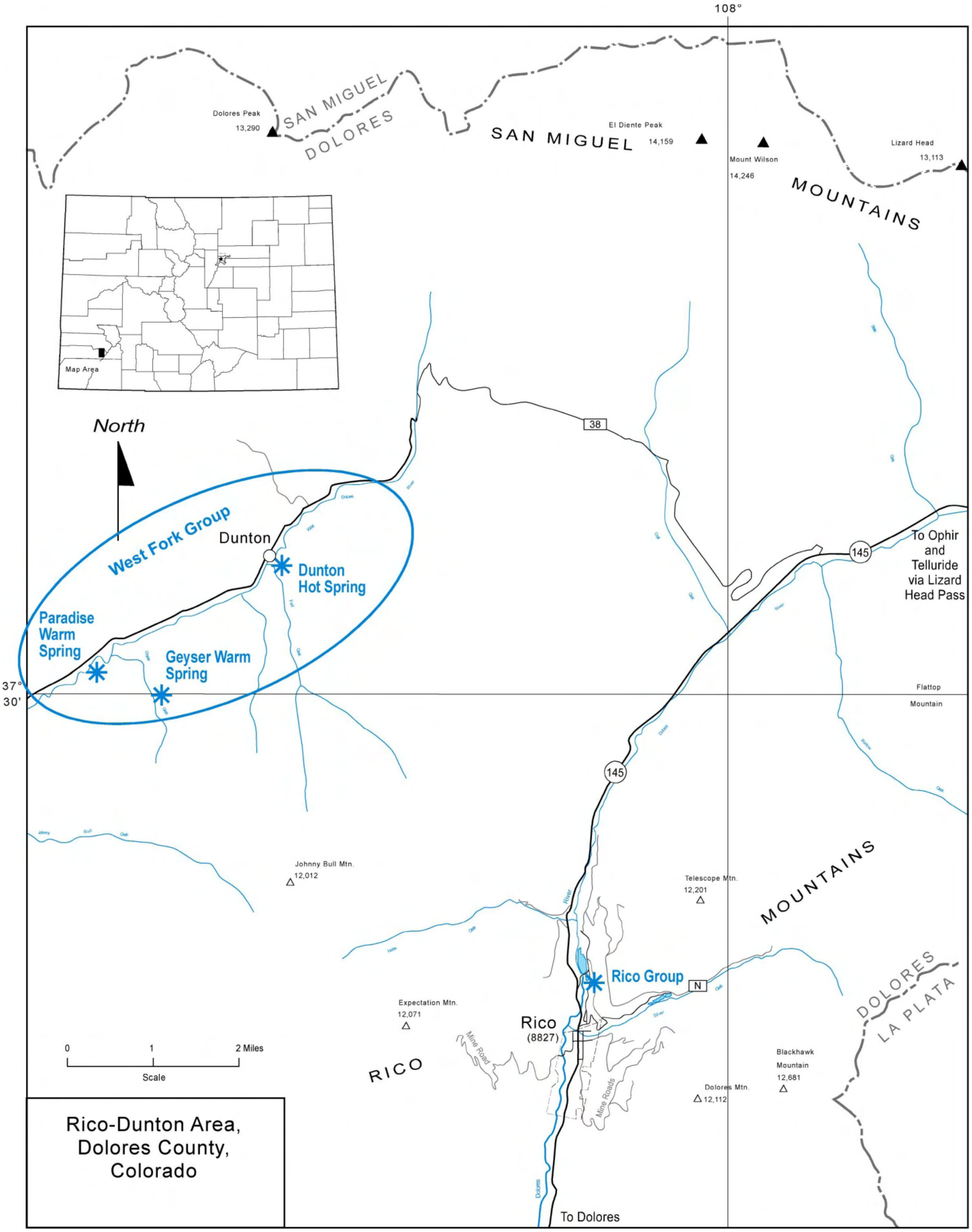

Figure 3. Map of study area near Rico, Colorado

2. Methods of Investigation

During the course of this investigation, six thermal springs were visited in July 2008 and field measurements of temperature, pH, conductivity, dissolved oxygen, and alkalinity were made. Samples were collected for chemical and isotopic analysis. Previous hydrologic and geochemical data from Barrett and Pearl (1976), for flowing drill holes in the Rico area and warm springs in the West Fork Dolores area, were also used in this study. The following sampling and measurement methodology was employed for each site.

Water was sampled in a two-step process: two liters of spring water were collected and then brought to a suitable sub-sampling location where the bulkier sampling equipment (Figures 4 and 5) was located. All samples collected during the course of this investigation were handled according to the protocols described in Appendix A (Sampling Methods). These protocols follow standard methods for dissolved and total recoverable fractions for cations, anions, and chemical constituents, with the addition of a cooling coil (Figure 5) designed to enhance preservation of dissolved CO_2 in the sample water.

Water samples were analyzed for the following:

- Chemical constituents silica, carbon dioxide, and sulfide;
- Ionic species chloride, fluoride, nitrate, phosphate, sulfate, bicarbonate, carbonate, and hydroxide;
- Elements including aluminum, antimony, arsenic, barium, beryllium, boron, cadmium, calcium, chromium, cobalt, copper, iron, lead, lithium, magnesium, manganese, mercury, molybdenum, nickel, phosphorus, potassium, selenium, silicon, silver, sodium, strontium, thallium, tin, titanium, vanadium, and zinc; and
- Isotopes ^{2}H hydrogen (deuterium) and ^{18}O oxygen were also conducted.

The United States Geological Survey's PHREEQC (Parkhurst and Appelo, 1999) modeling code was used to examine the water samples' equilibrium state with respect to various chemical species of interest. The parameters and constituents useful for PHREEQC aqueous speciation modeling include temperature, pH, CO_2 content, alkalinity, calcium, sodium, potassium, magnesium, chloride, iron, silica, nitrate, aluminum, boron, barium, cadmium, copper, lithium, manganese, phosphorus, lead, strontium and zinc.

To determine a subsurface temperature, various geothermometers were used. Silica based geothermometers require a silica (SiO_2) concentration in parts per million (ppm). Various cation geothermometers require concentrations of sodium, potassium, magnesium, lithium, and calcium in parts per million. In addition, the CO_2 correction to the sodium-potassium-calcium geothermometer requires an analysis for CO_2. Isotopic geothermometers used in this study require the measurement of ^{2}H (deuterium) and ^{18}O in parts per thousand (‰).

All chemical analyses for the July 2008 sampling event were performed by Huffman Laboratories in Golden, Colorado. Isotopic analyses for this sampling event were performed by the Colorado School of Mines Stable Isotope Laboratory in Golden, Colorado. Chemical analyses for the 1975 and 1976 samples were performed at the United States Geological Survey Central Laboratory in Salt Lake City, Utah.

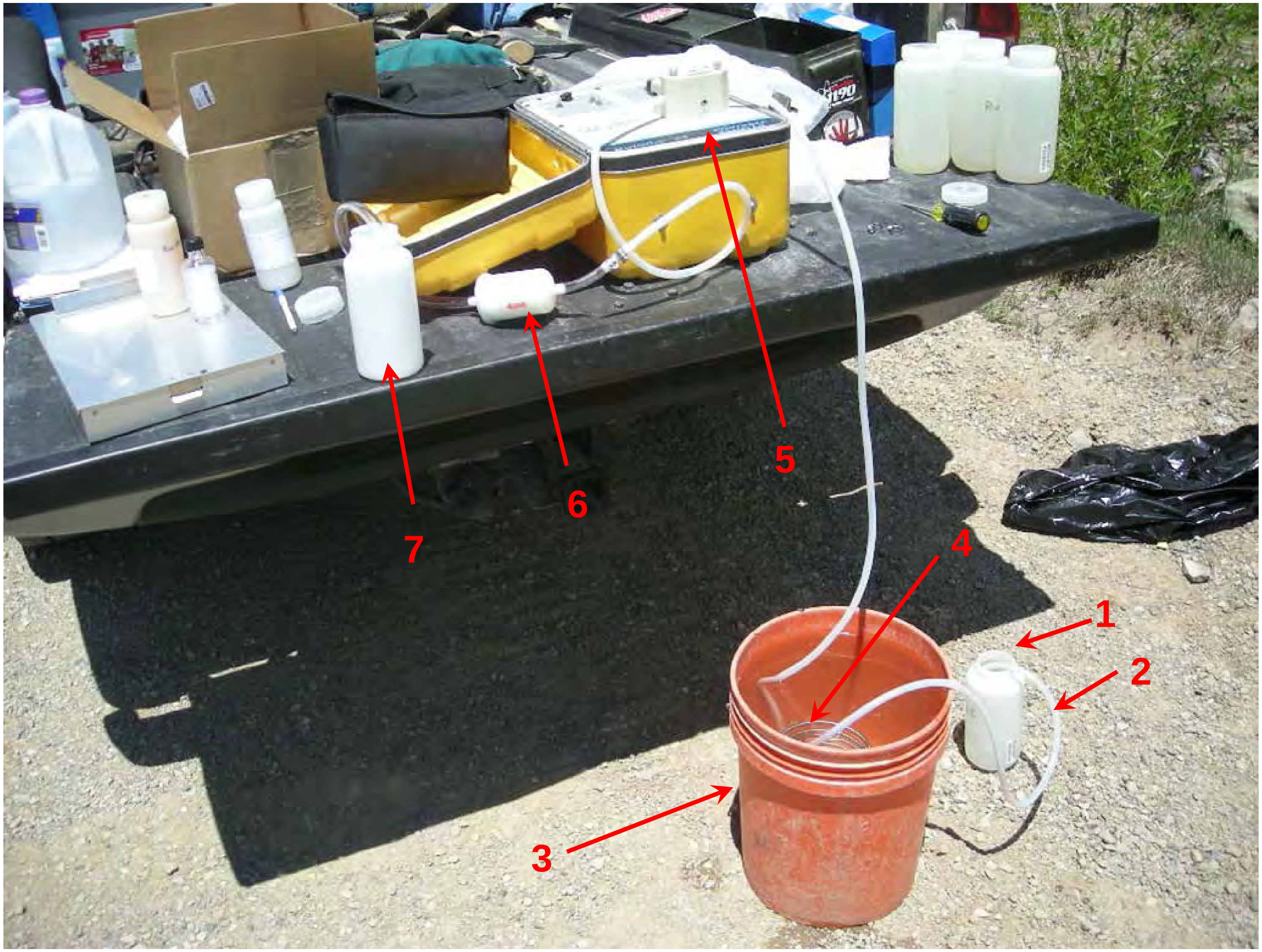

Figure 4. Sub-sampling equipment used in this study. 1) Bulk sample bottle 2) Tubing compatible with cooling coil, 3) Plastic bucket filled with ice and water, 4) Cooling coil, 5) Sampling pump, 6) 0.45µ filter, 7) Receiving sample bottle. For detailed sampling protocols, see the Appendix.

Figure 5. Stainless steel cooling coil, which is immersed in a bucket filled with ice and water during sampling. The brass fitting visible in the photo is a union fitting that allows two pieces of tubing to be joined together to form a longer (~16 ft), continuous coil.

3. Site Descriptions

3.1 Rico Group

The Rico Group consists of three thermal springs and up to four flowing drill holes approximately 0.5 mile north of the Town of Rico (Figure 6). Barrett and Pearl (1976 and 1978) reported results for samples collected from four flowing drill holes, likely drilled for mineral exploration. The date these holes were drilled and their depths are not known. The four drill holes reported in the 1976 and 1978 studies are discussed as all being located along the eastern side of the Argentine Mine access road. Cappa and Hemborg (1995) also utilized the Barrett and Pearl results for the Rico drill holes. Cappa and Hemborg reported that two of the four holes were uncapped and flowing water. In 2010, two of the drill holes were locatable. This group of drill holes is referred to as the Rico Drill Hole Group in this report. The Rico Springs Group is comprised of the three surface springs sampled in July 2008, and a simple numbering system was employed to designate these springs as shown in Figure 6.

The geology and structure in the area of the Rico Group is complex. Numerous rock types and ages from Precambrian metamorphic rocks to Mississippian and younger sedimentary rocks are juxtaposed against each other (Figures 7 and 8). Structurally, the area contains numerous east-west trending faults and the Rico Dome that trends east-west across the area. These large-scale structural features may play a role in creating preferential flow paths for deep circulation and heating of water (Barrett and Pearl, 1978). In addition to the large-scale structure are smaller scale fractures (creating individual blocks several inches in length within rock masses) that may allow for faster mixing and dilution of thermal and non-thermal water.

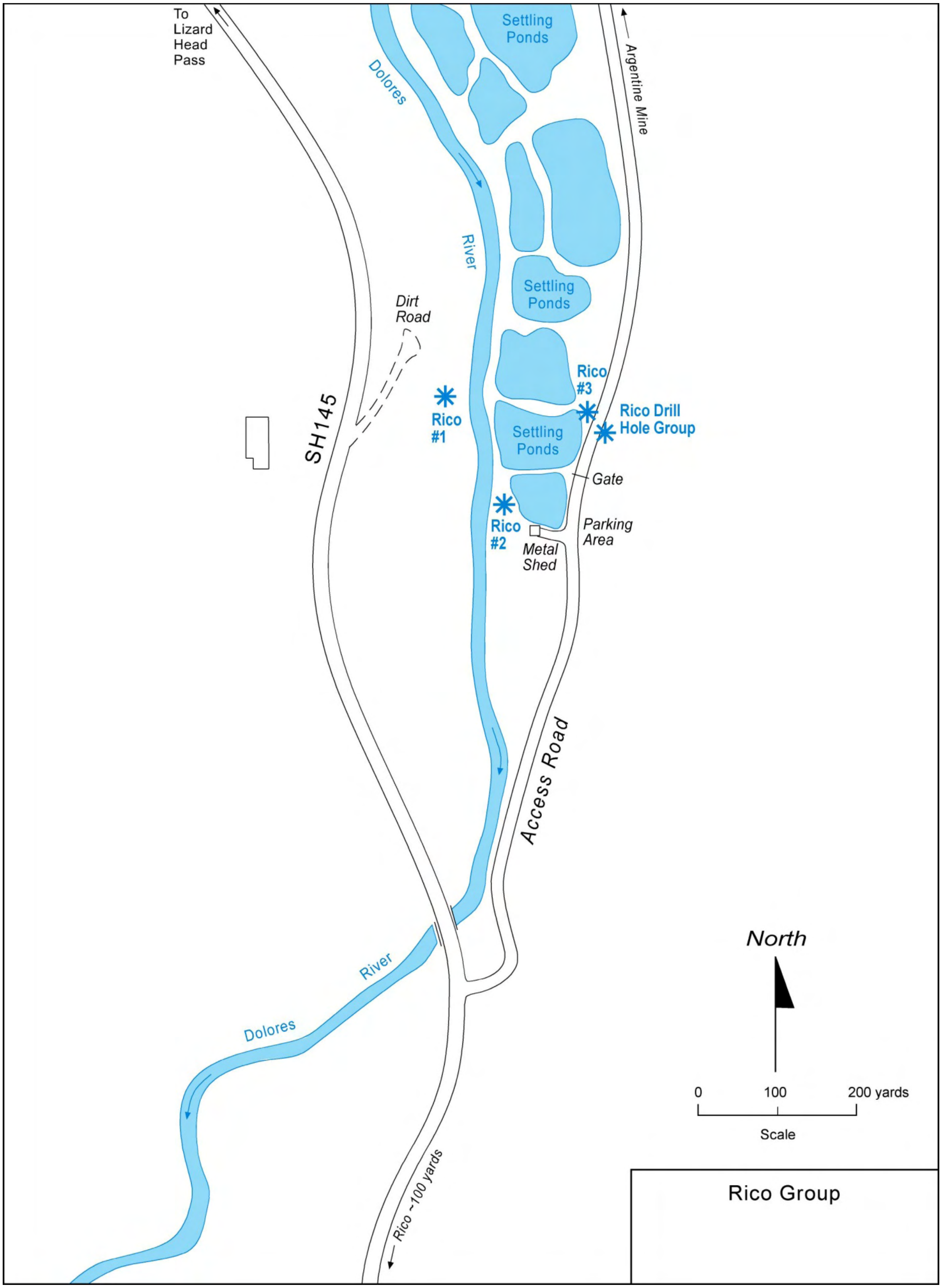

Figure 6. Map of the Rico Group area

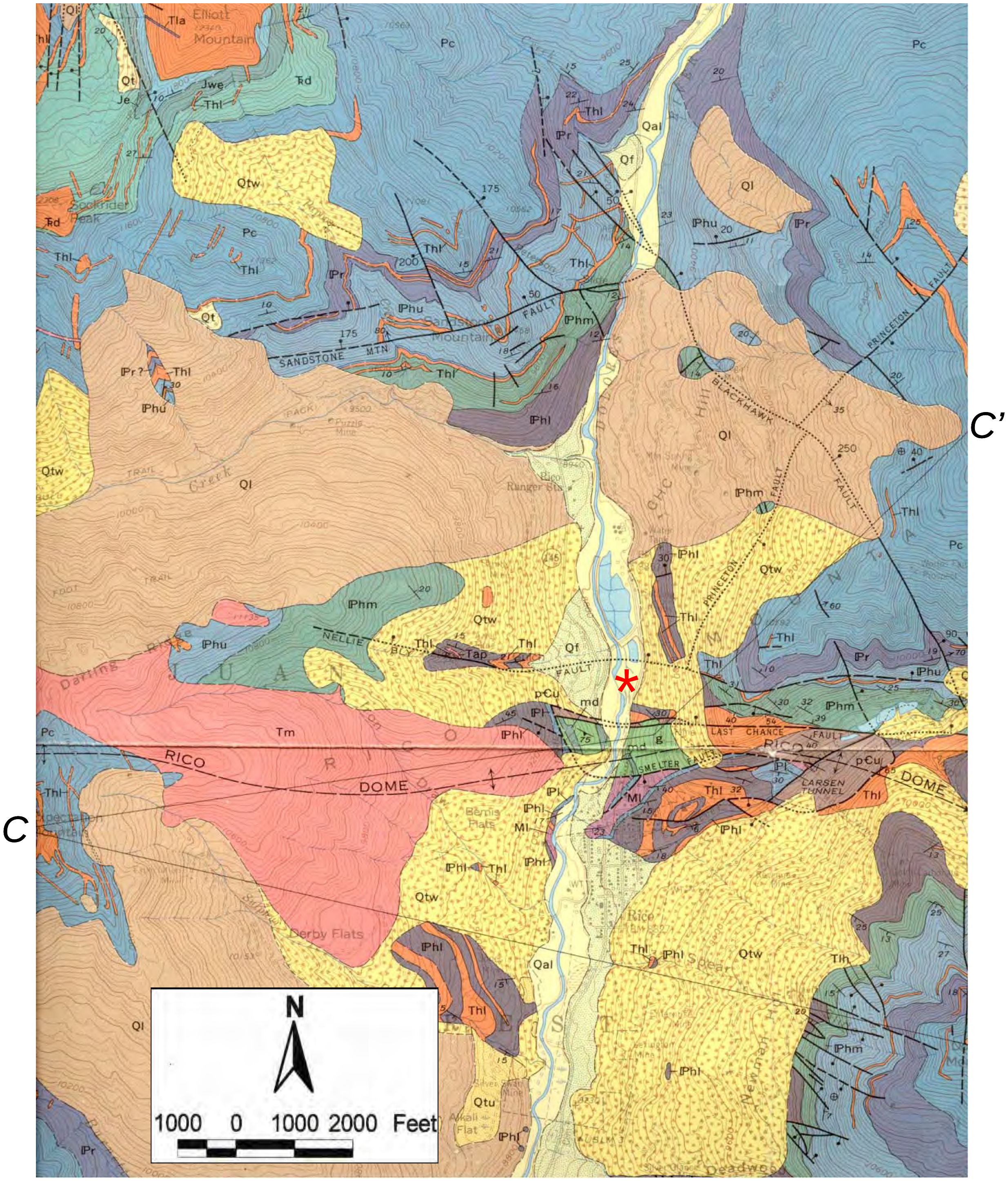

Figure 7. Geologic map of the Rico area. Cross section C-C' (shown in Figure 10) runs just south of the Rico Group (red asterisk). Map legend on next page (Pratt et al, 1969).

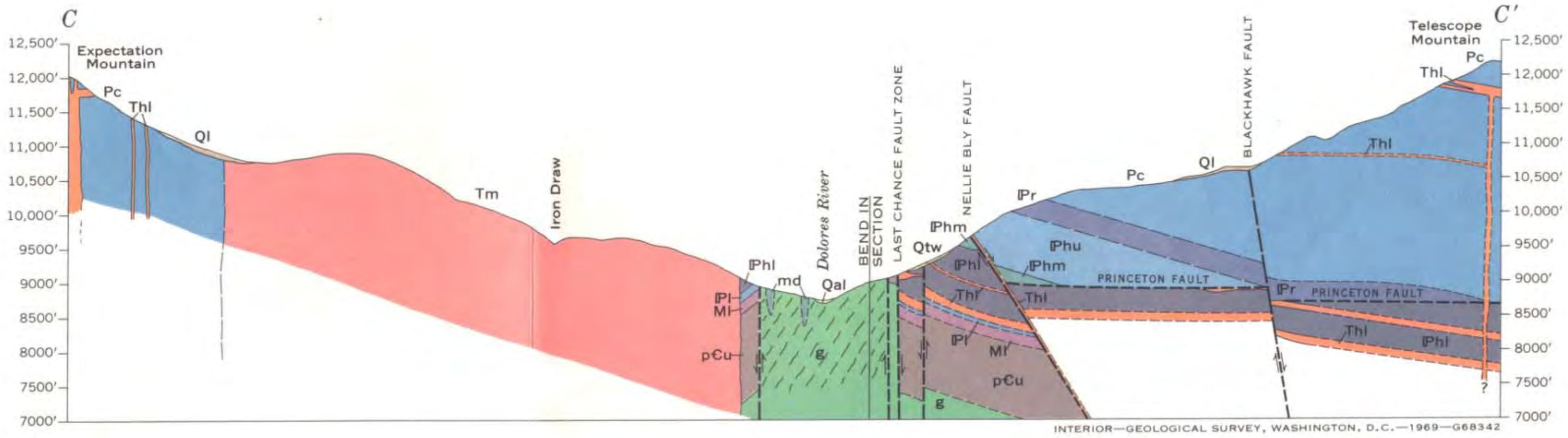

Figure 8. Cross section *C-C’* from Figure 7 (Pratt et al, 1969).

Explanation of geologic map symbols in Figures 7 and 8 (from Pratt et al, 1969).

Qal=Quaternary alluvium
Qf=Quaternary torrential fans
Qtw=Quaternary talus and slopewash
Qt=Quaternary talus
Qw=Quaternary slopewash
Ql=Quaternary landslide deposits
Qtu=Quaternary calcareous tufa
Qd=Quaternary glacial drift
Tcl=Tertiary porphyritic biotite-hornblende latite of Calico Peak Porphyry
Tca=Tertiary altered porphyritic biotite-hornblende latite of Calico Peak Porphyry
Tla=Tertiary augite lamprophyre
Tlh=Tertiary hornblende lamprophyre
Tb=Tertiary basalt
Tap=Tertiary alaskite
Tal=Tertiary porphyritic augite latite
Tm=Tertiary augite monzonite
Thl=Hornblende latite porphyry

Kd=Cretaceous Dakota Sandstone
Jmb=Brushy Basin shale member of Jurassic Morrison Formation
Jms=Salt Wash sandstone member of Jurassic Morrison Formation
Jw=Jurassic Wanakah Formation
Jwe=Jurassic Wanakah Formation and Entrada Sandstone
Je=Jurassic Entrada Sandstone
TR=Triassic Dolores Formation
Pc=Permian Cutler Formation
ℙr=Pennsylvanian Rico Formation
ℙhu=upper member of Pennsylvanian Hermosa Formation
ℙhu=middle member of Pennsylvanian Hermosa Formation
ℙhu=lower member of Pennsylvanian Hermosa Formation
ℙl=Pennsylvanian Quartzite of Larsen tunnel area
Ml=Mississippian Leadville Limestone
p€u=Precambrian Uncompahgre Quartzite
p€md=Precambrian metadiorite
g=Precambrian greenstone

3.1.1 Rico #1 Thermal Spring

Rico #1 is located along the west bank of the West Fork Dolores River and to the east of SH 145 (Figure 6) (UTM coordinates Northing: 4176891, and Easting: 12761735). Access to Rico Spring #1 is via a small parking area on the east side of State Highway (SH) 145, approximately 0.5 mile north of the SH 145 bridge over the Dolores River. The turnout for this parking area is directly across SH 145 from a highway maintenance facility. A short foot trail descends down to the spring situated on the west bank of the Dolores River.

Rico #1 thermal spring created a precipitate apron that is approximately 50 x 80 ft in areal extent (Figure 9). The spring pool at the outlet of the spring is approximately 6 ft in diameter with an unknown depth (Figure 10). An additional precipitate mound sits directly atop the spring outlet and stands approximately 3 ft high (Figure 11). Spring water consistently flows upward from beneath the taller precipitate mound. The spring pool is consistently out-gassing and there is periodic strong out-gassing from within the main precipitate mound every 2-5 seconds. The strong out-gassing escapes from multiple vents on the taller precipitate mound and produces a spray of spring water from some of the vents. Additionally, numerous gas seeps from the north side of the larger precipitate mound have consistent out-gassing.

During this investigation spring water was sampled from the edge of the spring pool and the water had a temperature of 40.8ºC. The discharge of the spring was not measurable due to the configuration of the pool and the multiple outfalls from the spring pool, all of which were very wide and shallow. A visual estimate of the discharge was approximately 5 gpm. Various hydrologic parameters are given in Table 1 (page 33). The water in the spring pool was somewhat clear with a greenish color. Abundant algae were observed in the pool.

Figure 9. View of Rico #1 looking southeast with Dolores River in background.

Figure 10. Rico #1 spring pool is approximately 6 feet in diameter.

Figure 11. Rico #1 precipitate mound, dark spots on mound are degassing vents.

3.1.2 Rico #2 Thermal Spring

Rico #2 is located across a settling pond from the parking area along the access road to the Argentine Mine (Figure 6). Access to Rico Springs #2, #3 and the drill-hole group is via a dirt access road that intersects with SH 145 just south of the bridge that carries SH 145 across the Dolores River. This dirt road runs north and into property associated with the Argentine Mine. Approximately 300 yards north along the access road there is a small parking area adjacent to a small metal shed. A gate crosses the access road just north of the parking area. The spring outlet is approximately 10 ft from the western edge of the lowermost settling pond and approximately 20 ft east of the Dolores River (UTM coordinates Northing: 4176794 and Easting: 12761800) (Figure 12).

The spring pool is approximately 6 ft in diameter with an unknown depth and has been created both by the spring's upwelling and by the piling of rocks around the perimeter of the pool (Figure 13). The spring has a constant out-gassing with a vigorous bubbling action. There is no noticeable odor associated with this spring. There is abundant orange and red precipitate around the spring and it sits atop a precipitate mound approximately 20 ft in diameter (Figure 14). Numerous gas seeps are consistently out-gassing along the precipitate apron down along the edge of the pond. A pipe directs some of the spring water out of the spring pool and down into a human-made soaking tub that is used for recreation (Figure 15).

During this investigation, water was sampled from the northern edge of the spring pool immediately adjacent to the out-gassing source and the water had a temperature of 42.8ºC. The discharge of the spring was not measurable due to the configuration of the pool and the multiple outfalls from the spring pool, all of which were very wide and shallow. A visual estimate of the discharge was approximately 5 gpm. Various hydrologic parameters are given in Table 1 (page 33). The water in the spring pool was mostly clear.

Figure 12. View of Rico #2 looking to the northwest. Rico #1 is visible in the background, on the right side of the photograph.

Figure 13. Rico #2 spring with precipitate apron. Numerous gas seeps are present along the edge of the apron and are issuing through approximately 4 inches of pond water.

Figure 14. Rico #2 spring pool is approximately 6 feet in diameter.

Figure 15. Bathing area approximately 50 feet from Rico #2. Water from Rico #2 is fed to soaking tub by the white pipe visible above the tub.

3.1.3 Rico #3 Thermal Spring

Rico #3 is located immediately off of the western shoulder of the Argentine Mine access road, approximately 100 ft north of the gate (Figure 6) (UTM coordinates Northing: 4176877 and Easting: 12761866). Rico #3 sits atop a yellow, white, and red precipitate mound that stands approximately 3 ft above the access road and 10 ft above the settling ponds below (Figure 16). The spring pool is approximately 2 ft in diameter (Figure 17). The water is mostly clear with no insect life present. Green algae are abundant where the spring discharge runs off the precipitate mound. A constant minor out-gassing in the spring pool is punctuated by a more vigorous out-gassing at 20 to 30 second intervals with duration of approximately 10 to 20 seconds. This vigorous out-gassing produces a minor geyser action which reaches heights of approximately 6 inches above the quiescent level of the spring pool (Figure 18). There is no noticeable odor associated with this spring. Water was sampled from the spring pool and had a temperature of 41.1ºC. The discharge of the spring was not measurable due to the configuration of the pool and the outfall from the spring pool, which is very shallow. A visual estimate of the discharge was less than 1 gpm. Various hydrologic parameters are given in Table 1 (page 33).


Figure 16. Rico #3 as seen from the access road, view is looking southwest.


Figure 17. Rico #3 spring pool is approximately 2 feet in diameter.

Figure 18. Photos of Rico #3 when placid (top) and when out gassing and "geysing" (bottom).

3.1.4 Rico Drill Hole Group

The Rico Drill Hole Group is adjacent to the eastern shoulder of the Argentine Mine access road, approximately 60 ft north of the gate (Figure 6) (UTM coordinates Northing: 4176863 and Easting: 12761874). At the time of the sampling event for this investigation (2008), one of the drill holes had a horizontal pipe connected to the vertical pipe emerging from the ground. This horizontal pipe was coupled to a hose that runs under the ground surface to the north (Figures 19 and 20). It is not apparent where the hose runs or the eventual fate (use?) of the thermal water it carries. There is a leak in the pipe-hose junction and water is intermittently escaping at this joint. The escaping water appears to be under pressure and spurts out periodically. In 2010, another capped drill pipe was located in the immediate vicinity. No samples were collected from the Drill Hole Group in the 2008 sampling event because no flowing water was accessible.

Figure 19. Photograph of the visible pipe of Rico Drill Hole Group taken from access road, view is to the south. Note access gate in background.

Figure 20. Close up photograph of Rico Drill Hole Group pipe, note junction of horizontal pipe with sloping hose. The precipitate on the ground is formed from leaking water at the pipe-hose junction.

3.2 West Fork of the Dolores River Group Site Descriptions

Along the West Fork of the Dolores River are two warm springs, Dunton and Paradise, and another spring is located along Geyser Creek, approximately 1.5 miles from the river (Figure 3). Access to the area is via Dolores County Road 38 which turns west off State Highway 145, approximately two miles north of Rico. It forms a 28-mile loop back to SH 145 intersecting just south of the town of Stoner. The southern portion of the County Road 38 loop is paved from the intersection with SH 145 (Stoner) north approximately 15 miles. The northern nine miles of the road to the intersection with SH 145 (north of the Town of Rico) is unpaved with numerous switchbacks and narrow sections. It was in varied condition in 2008.

3.2.1 Dunton Hot Spring

Dunton Hot Spring is located in the historic mining town of Dunton, which is now a private resort. Dunton is located approximately 20 miles north of the southern intersection of CR 38 and SH 145 (Figure 3). Dunton Hot Springs Resort consists of the town of Dunton's historic structures, which have been restored. The Dunton Spring is located at the base of the hill east of the main buildings (Figures 21 and 22) (UTM coordinates Northing: 4184508, and Easting: 12756024). Upwelling waters from Dunton spring are contained within a man made wooden cistern surrounded by a wooden deck structure (Figures 23 and 24). This arrangement allows bathing in the cistern. The waters are piped approximately 100 feet to a building where they empty into a large pool and are used for bathing. From this pool, the waters drain to the West Dolores River.

During this investigation the spring water was sampled from the edge of the cistern immediately adjacent to the wooden stairs that descend into the pit. The water had a temperature of 41.4º C. The discharge of the spring was not measurable due to the configuration of the cistern and the inaccessible location of the outfall discharge into the bathhouse pipe. Various hydrologic parameters are given in Table 2 (page 34). Water in the spring pool was somewhat clear with a greenish color. No insects or algae were observed in the cistern. The cistern pool had a nearly constant out-gassing occurring from below, that could be qualitatively described as minimal to moderate, and without lapse. No precipitate was present in the wooden cistern, possibly due to cleaning by resort personnel. There was no odor associated with the spring water or evolving gasses.

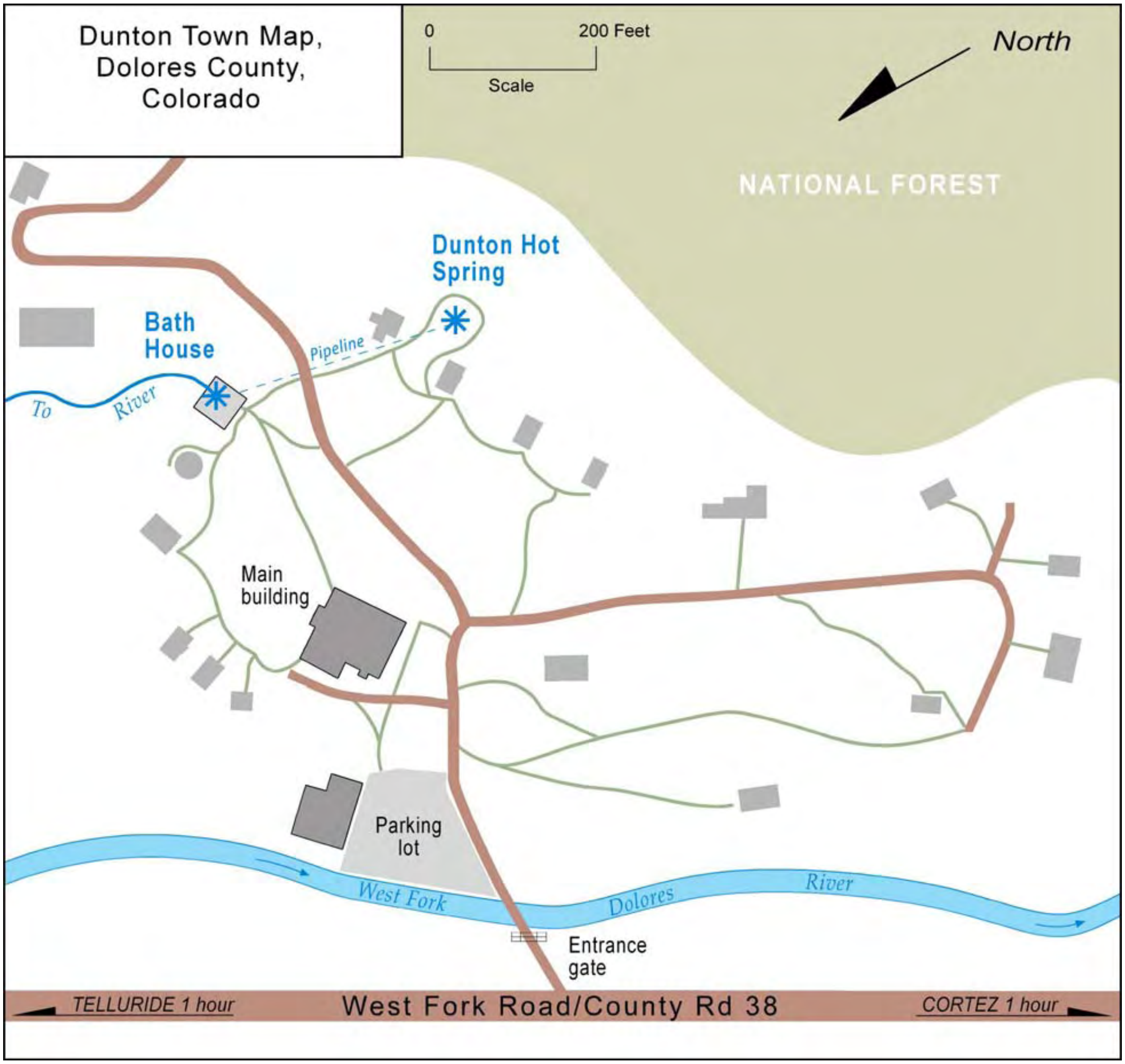

Figure 21. Map of the Town / Resort of Dunton

Figure 22. Dunton Spring is located between the two cabins.

Figure 23. Dunton Spring with surrounding wood deck.

Figure 24. View down into Dunton Spring cistern. Note disturbance of water surface from continuous out-gassing.

Red sandstones, siltstones, and shales of the Dolores Formation comprise the bedrock surrounding Dunton (Figure 25). As shown on the accompanying geologic map (Figure 25), several major north-northwest trending faults, with major displacement, pass through or are located only a short distance from Dunton. The fault on which the Dunton Hot Spring is located has dropped the Morrison Formation down into contact with the Entrada and Dolores Formations (Barrett and Pearl, 1976, 1978).

Figure 25. Geologic Map of the West Fork of the Dolores Group area (after Bush and Bromfield, 1966).

Explanation of geologic map symbols in Figure 25 (after Bush and Bromfield, 1966).

Qal=Quaternary alluvium
Qt=Quaternary talus
Ql=Quaternary landslide deposits
Qtu=Quaternary calcareous tufa
Qd=Quaternary glacial drift
Tl=Tertiary hornblende lamprophyre
Tm=Tertiary microgabbro
Kd=Cretaceous Dakota Sandstone

Km-Mancos Shale
Jmb=Brushy Basin shale member of Morrison Formation
Jms=Salt Wash sandstone member of Morrison Formation
Jw=Jurassic Wanakah Formation
Je=Jurassic Entrada Sandstone
Trd=Triassic Dolores Formation
Pc=Permian Cutler Formation

3.2.2 Geyser Warm Spring

Geyser Warm Spring is reached via Forest Service Trail #648 (Geyser Springs Trail), whose trailhead is located along Dolores County Road 38 approximately 2 miles south of Dunton (Figure 26) (UTM coordinates: 4182971 Northing, 12753092 Easting). There is a small parking area at the trailhead on the east side of County Road 38. The trail crosses the Dolores River 300 yards from trailhead. Approximately 1.3 miles from the trailhead, the trail forks and the right-hand fork leads downhill to the spring. Geyser Warm Spring is located approximately 500 yards down this trail adjacent to Geyser Creek (UTM coordinates Northing: 4182191, and Easting: 12753694) (Figure 27).

This spring has been described, as implied by its name, as a true geyser and claimed to be the only true geyser in the State of Colorado. The duration of the geysing event witnessed was approximately 5 minutes. The geyser action is slight and boils only 6 to 8 inches above the static level of the spring pool. Barrett and Pearl, 1978, report the frequency of the eruption as 30 minute intervals. A second geysing event was not witnessed during this investigation, so the recurrence interval is not known, but is at least 40 minutes. When not geysing, numerous locations on the spring pool's surface exhibit streams of gas bubbles. The outgassing is "strong" and appears to hold constant in location and quantity of gas discharge. There is a moderate sulfur odor associated with the spring.

The spring pool appears to have been constructed out of rocks and likely forms a larger pool than its natural occurrence. Cementation of the surrounding rocks due to precipitation of minerals from the spring water is evident (Figure 28). The discharge of the spring was not measurable due to the configuration of the pool and its numerous outfalls down to the creek. When not geysing, there is no discharge of water from the spring pool to the creek (Figure 28); when geysing, the discharge from the spring pool to the creek was estimated to be 5-10 gallons per minute (Figure 29). Barrett and Pearl, 1978, describe the geyser action as achieving heights of 12 to 15 inches, but this observation may not be comparable to present conditions given the likely change in static water level in the spring pool relative to the spring outlet.

The spring pool was sampled from the downhill edge of the pool and the water temperature was 28.5ºC. The water temperature was not affected by the geysing event. Various hydrologic parameters are shown in Table 2 (page 34). The water in the spring pool was very murky and white to green in color. There was abundant white precipitate and green algae present on the rocks around the edge of the spring pool.

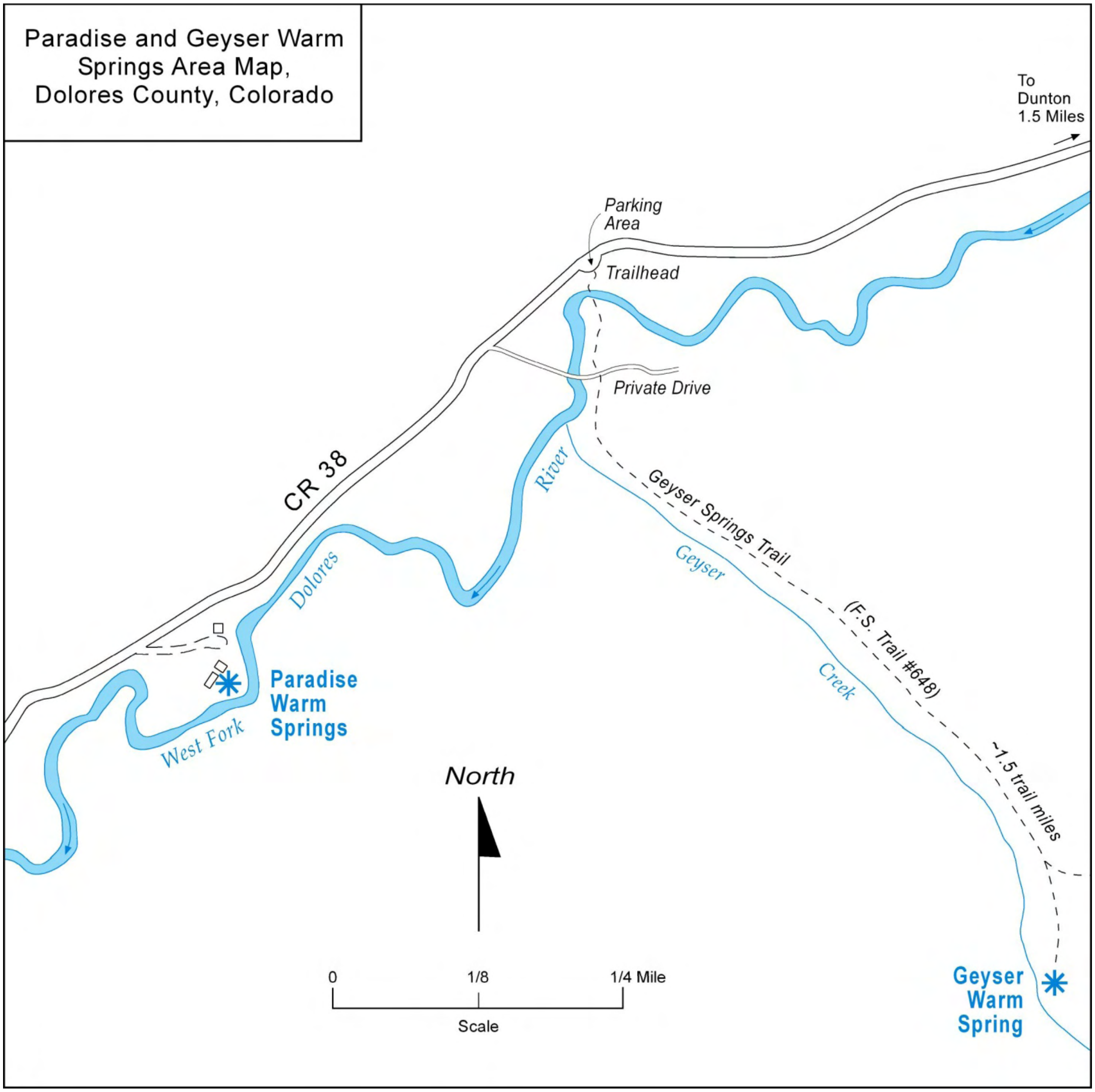

Figure 26. Map of the Geyser Warm Spring and Paradise Spring Area.

Figure 27. Geyser Warm Spring as seen from trail.

Figure 28. Geyser Warm Spring pool, note hat on right for scale.

Figure 29. Geyser Warm Spring at most vigorous geysing action, compare with previous photo of placid waters (Figure 40).

Bush and Bromfield (1966) have mapped the location of this spring near the intersection of two faults. A northeast-trending fault and a postulated northwest-trending fault may be controlling the location and formation of the Geyser Creek drainage in which Geyser Warm Spring is located (Figure 25). The waters emerge from the Dolores Formation, which overlies the Pennsylvanian Cutler Formation. The Dolores Formation consists of red siltstones, sandstone, shale, and a few limestone-pebble conglomerate beds (Bush and Bromfield, 1966). The intense faulting in the area makes reliable predictions of the recharge areas difficult (Barrett and Pearl, 1978).

3.2.3 Paradise Warm Spring

Paradise Warm Spring is located approximately 2.5 miles south of Dunton between the West Fork Dolores River and Dolores County Road 38 (Figures 3 and 26) (UTM coordinates Northing: 4182393, and Easting: 12752630). The spring pool is located in a bath house building to the east of the main cabin (Figure 30). The spring pool is contained within a cistern constructed of concrete and lined with wood logs and sheeting (Figure 31). Barrett and Pearl, 1978, report that the meadow between the buildings and the West Fork of the Dolores River has several small spring seeps, but none were visible during the July 2008 sampling event. Conversations with the occupant of the property indicate that the ground surface in this meadow remains warmer than the surrounding area, especially during the winter. Snow will not collect in the meadow when there is ample snow on the surrounding terrain. The bath house has an unfinished concrete swimming pool immediately adjacent to it. The unfinished swimming pool is a result of efforts by a previous owner during the 1950's to construct a spring-heated swimming pool. When blasting for the pool's foundation changed the spring flow, work was halted immediately. After approximately one year the spring waters re-emerged (Billy Moffat, personal correspondence, July 2008).

During this current investigation the spring water was sampled from the edge of the cistern and the water had a temperature of 43.4ºC. The discharge of the spring was not measurable due to the configuration of the cistern and the low flow of the outfall discharge into the West Fork Dolores, but was estimated to be approximately 1 gpm. Hydrologic parameters are given in Table 2 (page 34). The water in the spring pool was somewhat clear with a greenish color. No insects or algae were observed in the cistern. The cistern pool had a nearly constant out-gassing that could be qualitatively described as minimal. Minor red precipitate was present in the wooden cistern. No odor was associated with the spring water or out-gassing.

No published 7.5-minute geologic quadrangle maps exist for this area, but the geology of the Paradise Warm Springs area can be inferred from nearby published reports. It is likely that some of the northwest-southeast trending faults mapped in the area of Dunton and Geyser Warm Springs are indicative of the regional structure and a similar situation may be present in the Paradise Springs area (Figure 25). The spring waters emerge through West Dolores River alluvium which overlies the red sandstones, shales, and siltstones of the Cutler and Dolores Formations.

Figure 30. Bath house at Paradise Warm Spring. Note unfinished concrete swimming pool behind bath house. West Fork of the Dolores River is immediately behind bath house and pool.

Figure 31. Paradise Warm Spring pool inside bath house.

4. Results and Discussion

4.1 Water Chemistry Results

Hydrologic parameters and chemical analyses for the water samples collected in July 2008 as well as data from Barrett and Pearl, 1976, are shown in Tables 1 and 2. Rico Little Spring data from September 1975 are somewhat questionable with respect to the concentration of potassium listed in Barrett and Pearl, 1976. The 1976 study lists potassium as being present at the concentration of 5.6 mg/L which is not corroborated by a sample taken in January of 1976 which is reported as having a potassium content of 32 mg/L (Table 1, page 33). Potassium data for the other springs in the Rico group from the 1975-76 timeframe are in the 28-32 mg/L range. Charge balance calculations on the September 1975 data confirm a possible data problem with a 15% error in cation-anion balance. Typically, charge balance calculation errors in the 5% range are considered acceptable.

Table 1. Hydrological, chemical, and isotopic parameters for water samples from the Rico Group area. Chemical constituents listed are dissolved and passed through a 0.45μ filter (NM = not measured)

Constituent / Sample & Date	**Rico #1 7/08**	**Rico #2 7/08**	**Rico #3 7/08**	**Little Spring 9/75**	**Little Spring 1/76**	**Big Geyser 9/75**	**Big Geyser 4/76**	**Rico Geyser Warm Spring 9/75**	**Diamond Drill Hole 1/76**
Temperature (ºC)	40.8	42.8	41.1	38.0	39.0	34.0	36.0	38.0	44.0
Discharge (gpm)	NM	NM	NM	13	15	8	12	14	15
pH, Field	6.05	6.16	6.26	NM	7.00	NM	6.80	NM	7.00
Specific Conductance (mS)	2.66	2.55	2.82	4.70	3.35	3.25	3.10	3.20	2.71
Alkalinity (CaCO3) (mg/L)	1240	1140	1270	1400	1190	1390	1350	1420	919
Dissolved Oxygen (mg/L)	0.60	0.77	1.14	NM	NM	NM	NM	NM	NM
Chloride (Cl) (mg/L)	1	2	NM	2.3	3.0	4.1	4.3	3.9	2.4
Fluoride (F) (mg/L)	2	2	NM	1.5	4.8	2.1	1.5	2.1	1.4
Nitrate as NO3 (mg/L)	< 1.0	< 1.0	< 1.0	NM	NM	NM	NM	NM	NM
o-Phosphate as PO4 (mg/L)	< 2.0	2.0	< 2.0	0.25	0.34	0.25	0.55	0.28	0.25
Silica as SiO2 (mg/L)	133	128	135	120	120	110	140	110	120
Sulfate as SO4 (mg/L)	900	790	930	1000	960	900	920	920	810
Sulfide as S (mg/L)	< 2.0	< 2.0	< 2.0	NM	NM	NM	NM	NM	NM
Total CO2 as C (mg/L)	420	388	416	NM	NM	NM	NM	NM	NM
Bicarbonate as HCO3 (mg/L)	1510	1390	1550	1710	1450	1700	1650	1730	NM
Carbonate as CO3 (mg/L)	< 2.0	< 2.0	< 2.0	NM	NM	NM	NM	NM	NM
Hydroxide as OH (mg/L)	< 2.0	< 2.0	< 2.0	NM	NM	NM	NM	NM	NM
Aluminum (mg/L)	< 0.1	< 0.1	< 0.1	NM	NM	NM	NM	NM	NM
Antimony (mg/L)	< 0.05	< 0.05	< 0.05	NM	NM	NM	NM	NM	NM
Arsenic (mg/L)	0.020	0.030	0.027	0.026	NM	0.031	NM	0.026	NM
Barium (mg/L)	0.04	0.05	0.05	NM	NM	NM	NM	NM	NM
Beryllium (mg/L)	< 0.01	< 0.01	< 0.01	NM	NM	NM	NM	NM	NM
Boron (mg/L)	< 1.0	< 1.0	< 1.0	0.09	0.07	0.08	0.07	0.08	0.07
Cadmium (mg/L)	< 0.01	< 0.01	< 0.01	0	NM	1.0	NM	0	NM
Calcium (mg/L)	692.0	624.0	672.0	620.0	690.0	680.0	690.0	680.0	590.0
Chromium (mg/L)	< 0.01	< 0.01	< 0.01	NM	NM	NM	NM	NM	NM
Cobalt (mg/L)	< 0.05	< 0.05	< 0.05	NM	NM	NM	NM	NM	NM
Copper (mg/L)	< 0.05	< 0.05	< 0.05	NM	NM	NM	NM	NM	NM
Iron (mg/L)	5.0	6.5	3.3	4.8	7.4	8.3	8.5	8.5	0.0
Lead (mg/L)	< 0.001	< 0.001	< 0.001	NM	NM	NM	NM	NM	NM
Lithium (mg/L)	0.20	0.20	0.20	0.21	NM	0.25	NM	0.25	NM
Magnesium (mg/L)	89.0	90.0	100.0	110.0	92.0	98.0	93.0	100.0	82.0
Manganese (mg/L)	1.5	1.1	1.1	1.5	1.6	3.1	4.4	1.9	1.3
Mercury (mg/L)	< 0.002	< 0.002	< 0.002	0.001	NM	0.000	NM	0.000	NM
Molybdenum (mg/L)	< 0.1	< 0.1	< 0.1	NM	NM	NM	NM	NM	NM
Nickel (mg/L)	< 0.05	< 0.05	< 0.05	NM	NM	NM	NM	NM	NM
Phosphorus (mg/L)	< 0.5	< 0.5	< 0.5	NM	NM	NM	NM	NM	NM
Potassium (mg/L)	24.0	24.0	29.0	5.6*	32.0	30.0	31.0	32.0	28.0
Selenium (mg/L)	< 0.001	< 0.001	< 0.001	0	NM	0	NM	0	NM
Silicon (mg/L)	62.0	60.0	63.0	NM	NM	NM	NM	NM	NM
Silver (mg/L)	< 0.02	< 0.02	< 0.02	NM	NM	NM	NM	NM	NM
Sodium (mg/L)	66.0	62.0	74.0	76.0	77.0	78.0	67.0	80.0	66.0
Strontium (mg/L)	9.7	8.5	9.5	NM	NM	NM	NM	NM	NM
Thallium (mg/L)	0.001	0.001	0.001	NM	NM	NM	NM	NM	NM
Tin (mg/L)	0.17	0.12	0.13	NM	NM	NM	NM	NM	NM
Titanium (mg/L)	< 0.01	< 0.01	< 0.01	NM	NM	NM	NM	NM	NM
Vanadium (mg/L)	< 0.02	< 0.02	< 0.02	NM	NM	NM	NM	NM	NM
Zinc (mg/L)	0.03	0.08	0.05	0.10	NM	1.00	NM	0.08	NM
δ^{2}H (Deuterium) (‰ VSMOW)	-93.37	-93.68	-94.54	NM	NM	NM	NM	NM	NM
δ^{18}O (‰ VSMOW)	-12.912	-12.923	-12.962	NM	NM	NM	NM	NM	NM

Table 2. Hydrologic, chemical, and isotopic parameters for West Fork Group water samples. Chemical constituents listed are dissolved and passed through a 0.45µ filter (NM = not measured).

Constituent / Sample & Date	Dunton 9/75	Dunton 1/76	Dunton 4/76	Dunton 7/08	Geyser 9/75	Geyser 7/08	Paradise 9/75	Paradise 1/76	Paradise 4/76	Paradise 7/08
Temperature (ºC)	44.0	42.0	42.0	41.4	28.0	28.5	46.0	40.0	42.0	43.4
Discharge (gpm)	26	25	25	NM	NM	NM	26	34	30	NM
pH, Field	NM	7.00	6.40	6.05	NM	6.29	NM	6.90	6.80	6.40
Specific Conductance (mS)	1.85	1.89	1.86	1.42	2.50	2.24	9.56	10.70	10.00	8.98
Alkalinity (CaCO3) (mg/L)	719	828	837	780	1450	1060	515	562	572	579
Dissolved Oxygen (mg/L)	NM	NM	NM	1.24	NM	0.72	NM	NM	NM	1.41
Chloride (Cl) (mg/L)	6.6	6.3	7.0	< 1.0	2.4	< 1.0	3100.0	3300.0	3100.0	3190.0
Fluoride (F) (mg/L)	0.6	0.4	0.7	< 2.0	0.4	< 2.0	3.9	3.8	3.7	4.0
Nitrate as NO3 (mg/L)	NM	NM	NM	NM	NM	NM	NM	NM	NM	NM
o-Phosphate as PO4 (mg/L)	0.09	0.15	0.01	NM	0.28	NM	0.31	0.37	0.67	NM
Silica as SiO2 (mg/L)	34	32	33	39	37	43	150	200	150	169
Sulfate as SO4 (mg/L)	350	340	310	320	68	89	140	140	110	130
Sulfide as S (mg/L)	NM	NM	NM	< 2.0	NM	< 2.0	NM	NM	NM	< 2.0
Total CO2 as C (mg/L)	NM	NM	NM	309	NM	511	NM	NM	NM	184
Bicarbonate as HCO3 (mg/L)	877	1010	1020	951	1770	1300	628	685	697	706
Carbonate as CO3 (mg/L)	NM	NM	NM	< 2.0	NM	< 2.0	NM	NM	NM	< 2.0
Hydroxide as OH (mg/L)	NM	NM	NM	< 2.0	NM	< 2.0	NM	NM	NM	< 2.0
Aluminum (mg/L)	NM	NM	NM	< 0.1	NM	< 0.1	NM	NM	NM	< 0.1
Antimony (mg/L)	NM	NM	NM	< 0.05	NM	< 0.05	NM	NM	NM	< 0.05
Arsenic (mg/L)	0.005	NM	NM	0.010	0.000	< 0.001	0.140	NM	NM	0.112
Barium (mg/L)	NM	NM	NM	0.05	NM	0.41	NM	NM	NM	0.32
Beryllium (mg/L)	NM	NM	NM	< 0.01	NM	< 0.01	NM	NM	NM	< 0.01
Boron (mg/L)	0.09	0.11	0.09	< 1.0	0.12	< 1.0	9.30	1.00	4.30	10.00
Cadmium (mg/L)	0	NM	NM	< 0.01	0	< 0.01	0	NM	NM	< 0.01
Calcium (mg/L)	330.0	360.0	340.0	318.0	170.0	165.0	160.0	240.0	170.0	183.0
Chromium (mg/L)	NM	NM	NM	< 0.01	NM	< 0.01	NM	NM	NM	< 0.01
Cobalt (mg/L)	NM	NM	NM	< 0.05	NM	< 0.05	NM	NM	NM	< 0.05
Copper (mg/L)	NM	NM	NM	< 0.05	NM	< 0.05	NM	NM	NM	< 0.05
Iron (mg/L)	2.3	0.8	1.1	< 0.05	0.0	< 0.05	0.2	0.1	0.2	< 0.05
Lead (mg/L)	NM	NM	NM	< 0.001	NM	< 0.001	NM	NM	NM	< 0.001
Lithium (mg/L)	0.10	NM	NM	0.10	0.28	NM	9.60	NM	NM	9.00
Magnesium (mg/L)	45.0	43.0	45.0	43.0	40.0	38.0	27.0	30.0	28.0	30.0
Manganese (mg/L)	1.8	1.7	1.9	1.7	0.7	0.7	0.8	0.9	0.8	0.8
Mercury (mg/L)	0.000	NM	NM	< 0.002	0.000	< 0.002	0.001	NM	NM	< 0.002
Molybdenum (mg/L)	NM	NM	NM	< 0.1	NM	< 0.1	NM	NM	NM	< 0.1
Nickel (mg/L)	NM	NM	NM	< 0.05	NM	< 0.05	NM	NM	NM	< 0.05
Phosphorus (mg/L)	NM	NM	NM	< 0.5	NM	< 0.5	NM	NM	NM	< 0.5
Potassium (mg/L)	19.0	21.0	21.0	18.0	29.0	26.0	360.0	380.0	370.0	377.0
Selenium (mg/L)	0	NM	NM	< 0.001	0	< 0.001	0	NM	NM	< 0.001
Silicon (mg/L)	NM	NM	NM	18.0	NM	20.0	NM	NM	NM	79.0
Silver (mg/L)	NM	NM	NM	< 0.02	NM	< 0.02	NM	NM	NM	< 0.02
Sodium (mg/L)	35.0	34.0	34.0	31.0	400.0	390.0	1800.0	1900.0	1900.0	1940.0
Strontium (mg/L)	NM	NM	NM	3.7	NM	5.0	NM	NM	NM	3.3
Thallium (mg/L)	NM	NM	NM	0.001	NM	< 0.001	NM	NM	NM	0.014
Tin (mg/L)	NM	NM	NM	< 0.05	NM	< 0.05	NM	NM	NM	< 0.05
Titanium (mg/L)	NM	NM	NM	< 0.01	NM	< 0.01	NM	NM	NM	< 0.01
Vanadium (mg/L)	NM	NM	NM	< 0.02	NM	< 0.02	NM	NM	NM	< 0.02
Zinc (mg/L)	0	NM	NM	< 0.01	0	< 0.01	0.05	NM	NM	< 0.01
δ^{2}H (Deuterium) (‰ VSMOW)	NM	NM	NM	-91.76	NM	-105.65	NM	NM	NM	-73.66
δ^{18}O (‰ VSMOW)	NM	NM	NM	-92.28	NM	-14.144	NM	NM	NM	-12.692

4.2 Geothermometry Discussion

The concentration and ratios of various compounds and/or elements (constituents) in geothermal waters can be used to evaluate the temperature at which the waters have evolved. A number of different geothermometer models can be employed, but all are based on a similar underlying premise. In general, as a reservoir of water at some depth in the Earth reacts with the surrounding rock, it will attain some measure of equilibrium with the minerals in that rock. The extent to which equilibrium is reached depends on a number of factors including the kinetics of the particular reaction, reactivity of the wall rock, concentrations of the elements in the water, and residence time and temperature of the water in the reservoir (Fournier, 1977).

To use the composition of spring and well waters to estimate subsurface temperatures, several assumptions must be made and are inherent in all geothermometer models (Fournier, White and Truesdell, 1974):

1. Temperature-dependant reactions involving rock and water fix the amount of dissolved constituents in the water.
2. There is an adequate supply of all reactants.
3. There is equilibrium in the reservoir with respect to the constituents of interest.
4. No re-equilibration of the constituents occurs after the water leaves the reservoir and flows to the surface.
5. Either no mixing of different waters occurs during movement to the surface or evaluation of the results of such mixing is possible.

It is important to keep these assumptions in mind when using any geothermometer. In the case of the Rico area, every assumption listed has the potential to be unsatisfied. Assumptions 1 through 3 are extremely difficult to satisfy because of the unknown nature of the heat source and unknown location of the geothermal reservoir. Assumptions 4 and 5 are difficult to confirm because of the complex geology and unknown flow path of ascending thermal water on its way to the surface. This does not mean that a geothermometer estimate is not accurate or has no value; rather that it is an estimate in a system with a large set of variables and unknowns.

Three main categories of geothermometers are applicable to spring and well waters: silica based, cation based, and isotope based. Silica based geothermometers are derived from silica solubility, temperature, and pressure relationships determined either experimentally or based on field observations and data. Cation geothermometers are based on ratios between cations (principally Na, K, Mg, Li, and Ca) and the exchange reactions (between water and minerals) that control their concentrations in water. Isotope geothermometers are based on the fractionation of elements into isotopes among different compounds that are temperature dependant.

4.2.1 Silica Based Geothermometers

Silica (SiO_2) based geothermometers are based on solubility reactions between various silica phases (quartz, chalcedony, and amorphous silica) and water. Table 3 lists the various silica based geothermometers that were employed in this study. As an aid to determine the most appropriate silica geothermometer to apply to each particular water sample, the saturation indices produced by aqueous speciation modeling for the various silica phases were examined, as described in section 4.3.

The various silica geothermometers were then applied to the available data and estimated subsurface temperatures were generated. It is important to note that there can be several choices within a mineral group, i.e. six different geothermometers for quartz and two in the case of chalcedony. This has the effect of producing a range of subsurface temperature estimates. In this study, the approach was to evaluate all of the appropriate geothermometers and look for internal agreement within the group.

Table 3. Silica geothermometer equations used in this study (after D'Amore and Arnorsson, 2000).

Temperature Equations for the Silica Geothermometers
(*S* represents silica concentration as SiO_2 in mg/kg,
with concentrations of silica found in these waters mg/kg = mg/L = ppm)

Equation #	Geothermometer	Equation (T in °C)	Range (°C)	Source
1	Quartz	$\frac{1309}{5.19-\log S}-273.15$	25-250	Fournier (1977)
2	Quartz	$\frac{1522}{5.75-\log S}-273.15$	25-250	Fournier (1977)
3	Quartz	$-42.2+0.28831S-3.6686\times10^{-4}S^2$ $+3.1665\times10^{-7}S^3+77.034\log S$	25-900	Fournier and Potter (1982)
4	Quartz	$-53.5+0.11236S-0.5559\times10^{-4}S^2$ $+0.1772\times10^{-7}S^3+88.390\log S$	Not Reported	Fournier and Potter (1982)
5	Quartz	$-55.3+0.3659S-5.3954\times10^{-4}S^2$ $+5.5132\times10^{-7}S^3+74.360\log S$	0-350	Arnorsson et al. (1998)
6	Quartz	$-66.9+0.1378S-4.9727\times10^{-5}S^2$ $+1.0468\times10^{-8}S^3+87.841\log S$	0-350	Arnorsson et al. (1998)
7	Chalcedony	$\frac{1032}{4.69-\log S}-273.15$	0-250	Fournier (1977)
8	Chalcedony	$\frac{1112}{4.91-\log S}-273.15$	Not Reported	Arnorsson et al. (1983)

4.2.2 Cation Based Geothermometers

Cation geothermometers are based on the relative amounts of different cations in solution in geothermal water. Water present in a geothermal reservoir will undergo exchange reactions with the minerals present in the reservoir host rock and the water-rock system may approach equilibrium with respect to the constituent elements in the minerals. The relevant minerals present in these systems are highly varied across the range of hydrothermal systems, but are typically rock-forming minerals like feldspars (Na^+-bearing albite, K^+-bearing microcline, Ca^+-bearing anorthite) and micas.

The cation geothermometers used in this study are listed in Table 4. It may be noted that there are numerous cationic geothermometers available in the literature and those that contain similar cations differ with respect to their calibrations. This variance reflects the inherent variability in natural systems, the underlying thermodynamic data used in their derivation, and available empirical data. Again, it is necessary to use scientific judgment when considering various cationic geothermometers applied to a chemical dataset. One must view the range of geothermometric results in light of the geologic framework and consider the suitability of any particular geothermometer. Applied appropriately, consistency within a group of similar geothermometers lends credence to temperature estimates.

A number of corrections can be applied to the Na-K-Ca geothermometer, most notably a CO_2 correction (Paces, 1975) and a magnesium correction (Fournier and Potter, 1979). The CO_2 correction is listed on Line 13.1 in Table 9 (page 54). Note that the determination of the partial pressure of CO_2 used in this correction is estimated from the surface temperature of the water in question, and not from a direct laboratory measurement. The magnesium correction is not applicable to waters in the Rico area. The authors recommend that it not be applied to waters whose calculated Na-K-Ca temperature is less than 70º C of the correction (as in the case of the Rico Group and Dunton Spring) and whose resulting magnesium-correction temperature value is negative (as in the case of Paradise and Geyser Warm Springs) (Fournier and Potter, 1979).

Table 4. Cation geothermometer equations used in this study (after D'Amore and Arnorsson, 2000).

Temperature Equations for Cation Geothermometers
(Concentrations are in ppm if not otherwise specified,
with concentrations of cations found in this study ppm = mg/L = mg/kg)

Equation #	Geothermometer	Equation (T in ºC)	Range (ºC)	Source
1	K-Mg	$\frac{4410}{14.0-\log(K^2/Mg)}-273.15$	< 100	Giggenbach (1988)
2	Na-Ca	$\frac{1096.7}{3.08+\log(Na/Ca^{0.5})}-273.15$	Not Reported	Tonani (1980)
3	Na-K-Ca [Conc] in mol/kg B=4/3 for T<100ºC B=1/3 for T>100º and $\log(Ca^{0.5}/Na)<0$	$\frac{1647}{\log(Na/K)+\beta\log(Ca^{0.5}/Na)+2.24}-273.15$	Not Reported	Fournier and Truesdell (1973)

4.2.3 Isotope Based Geothermometers

Isotopic geothermometers are based on the fractionation of hydrogen and oxygen into different isotopes, specifically ^{16}O and ^{18}O, and ^{1}H and ^{2}H (where ^{2}H is commonly referred to as deuterium). Fractionation of these light elements is temperature dependant and thus these isotopes and their fractionation factors can constitute useful geothermometers. The fractionation of these stable isotopes is expressed in units of parts per mil deviation from a standard water known as the Vienna Standard Mean Oceanic Water (δ (Isotope) ‰ VSMOW). The isotope geothermometers used in this study are given in Table 5.

The methane – hydrogen gas geothermometer (Equation 1, Table 5) has been noted in several studies to give subsurface temperature estimates that are 20º C - 100º C higher than those measured in drill holes (D'Amore and Arnorsson, 2000). The water – hydrogen gas geothermometer (Equation 2, Table 3) has been used with good results and appears to be applicable to the Rico area. It is important to note that Equations 1 and 2 are based on isotope fractionation within gases. Measurement of isotopes in water that may or may not have equilibrated with incorporated gas adds another level of complexity regarding the isotopes in question.

Table 5. Isotopic geothermometers used in this study (after D'Amore and Arnorsson, 2000).

Temperature Equations for Isotopic Geothermometers
(with α=δ (Isotope) in ‰ VSMOW)

Equation #	**Reaction**	**Equation (T_K in Kelvin)**	**Source**
1	$CH_3D + H_2 =$ $HD + CH_4$ (methane - hydrogen gas)	$1000 \ln \alpha = 288.9 \times 10^3 / T_K + 31.86 \times 10^6 / T_K{}^2 - 238.28$ Valid in range 100 - 400° C	Bottinga (1969) Richet et al (1977)
2	$HD + H_2O =$ $H_2 + HDO$ (water - hydrogen gas)	$1000 \ln \alpha = 396.8 \times 10^3 / T_K + 25.196 \times 10^6 / T_K{}^2 - 284$ Valid in range 100 - 400° C	Richet et al (1977)

4.3 Water – Rock Interaction and Chemical Equilibrium

The crucial underlying assumption in any geothermometric analysis is the notion of a water attaining equilibrium with its surrounding rock and minerals. To evaluate critically the results of any estimate of subsurface temperature, the equilibrium state of the water needs to be considered.

As a first step in examining the equilibrium state of a water, geochemical aqueous speciation modeling is performed on each sample's analytical data using the modeling code PHREEQC (Parkhurst and Appelo, 1999), a publicly available code distributed by the United States Geological Survey (USGS). The PHREEQC output is used to evaluate the overall quality of the analytical data through evaluating the charge balance of the various ionic species. In general, a ±5% error is considered the threshold for a quality chemical analysis.

The saturation index of quartz and chalcedony are examined to determine each of the silica phase's saturation state, and therefore which polymorph is controlling the solution of silica into or precipitation out of the water. Saturation index is defined as:

$$SaturationIndex = SI = \log \frac{IAP}{K_{sat}}$$

where *IAP* is the Ion Activity Product of the ions in solution and K_{sat} is the equilibrium constant for the solution of a solid. When the ratio of the *IAP* and K_{sat} are equal to 1 (similar numbers), the *SI* is thus equal to 0, and the solution is said to be saturated with respect to the species in question and may be considered to be in equilibrium. When the *SI* is a positive number, the species is oversaturated and the species in question will tend to precipitate out of solution. When the *SI* is negative, the species is undersaturated and can dissolve into solution.

Table 6 lists the saturation indices for the water samples in this study. None of the water samples have a silica SI of exactly zero but are ±1 in general, indicating relative close proximity to equilibrium with the silica phases, and does not disqualify the silica geothermometers' utility in estimating a subsurface temperature, but rather provides a context in which to evaluate the geothermometry results. Departure from equilibrium may be due to either incomplete reaction of the water with surrounding silica phases, or may be due to dilution and mixing with different water, in this case shallow groundwater.

There is some inconsistency in the calculated saturation indices of the various silica minerals between the 1975 and 1976 samples and the 2008 samples. In general, the 2008 samples' silica content appears to be controlled by equilibrium with quartz and the 1970's samples are generally controlled by equilibrium with chalcedony. The samples that were collected in 2008 were analyzed for CO_2 content, while there is no CO_2 data available for the 1970's samples. Inclusion of CO_2 concentration data is a significant factor when modeling the chemistry data with PHREEQC. In general, when CO_2 data is included in the modeling, the resulting silica-controlling species is quartz. Without CO_2 data, chalcedony is calculated to have an SI closer to zero.

Table 6. Silica phase saturation indices for samples in this study. Asterisk indicates samples that have CO_2 data included in the PHREEQC speciation modeling.

Sample	Chalcedony	Quartz
Rico #1 7/2008*	-1.04	-0.66
Rico #2 7/2008*	-0.99	-0.61
Rico #3 7/2008*	-1.06	-0.68
Rico Little Spring 9/75	0.71	1.10
Rico Little Spring 1/76	0.70	1.09
Rico Big Geyser 9/75	0.72	1.12
Rico Big Geyser 4/76	0.80	1.20
Rico Geyser Warm Spring 9/75	0.68	1.07
Rico DDH 1/76	0.65	1.02
Dunton Spring 9/75	0.10	0.47
Dunton Spring 1/76	0.09	0.47
Dunton Spring 4/76	0.11	0.49
Dunton Spring 7/2008*	-1.35	-0.97
Geyser Warm Spring 9/75	0.31	0.73
Geyser Warm Spring 7/2008*	-1.31	-0.89
Paradise Spring 9/75	0.74	1.11
Paradise Spring 1/76	0.93	1.31
Paradise Spring 4/76	0.78	1.16
Paradise Spring 7/2008*	-0.35	0.02

Another approach to determine the equilibrium state of a water is to examine the relative concentrations of several chemical constituents and their relation to each other. Giggenbach (1988) used this approach in considering the reaction between water, Na^+-bearing albite and K^+-bearing microcline, and the reaction between water, these feldspars and Mg^{2+}-bearing micas and chlorite, to produce a trilinear diagram that represents various ratios of these three elements (Figure 32). When a water sample's concentrations of these three elements are plotted into this geoindicator diagram, it becomes possible to assess the water's equilibrium state with respect to Na, K, and Mg. The line of full equilibrium temperatures shown in the diagram is based on the selection of a Na-K geothermometer. In this study, the Na-K geothermometer of Arnorsson et al (1998) (Eqn #8 in Table 9, page 54) is used and was chosen because the underlying thermodynamic calibration data for this geothermometer is considered to be reliable (D'Amore and Arnorsson, 2000).

Points are plotted into the Na-K-Mg geoindicator diagram using the following relationships:

$$\frac{C_{Na}}{1000}+\frac{C_K}{100}+\sqrt{C_{Mg}}=S \qquad "\%-Na"=\frac{C_{Na}}{10S} \qquad "\%-Mg"=\frac{100\sqrt{C_{Mg}}}{S}$$

where C_X = Concentration of element *X (Na, K or Mg)* in mg/kg.

Figure 32 shows the Giggenbach geoindicator diagram with samples from this study plotted. The Rico Area and Dunton Spring samples plot very low in the magnesium corner of the diagram, indicating their lack of equilibrium with respect to the Na-K-Mg system. The

Geyser Warm Spring samples also plot low in the magnesium corner and exhibit a similar lack of equilibrium. The Paradise Spring samples plot higher in the partially equilibrated field and are interpreted to be closer in equilibrium in the Na-K-Mg system than the other spring groups. All of the samples plot in the partially equilibrated and mixed field which is indicative of their high degree of mixing with either non-equilibrated or non-thermal waters.

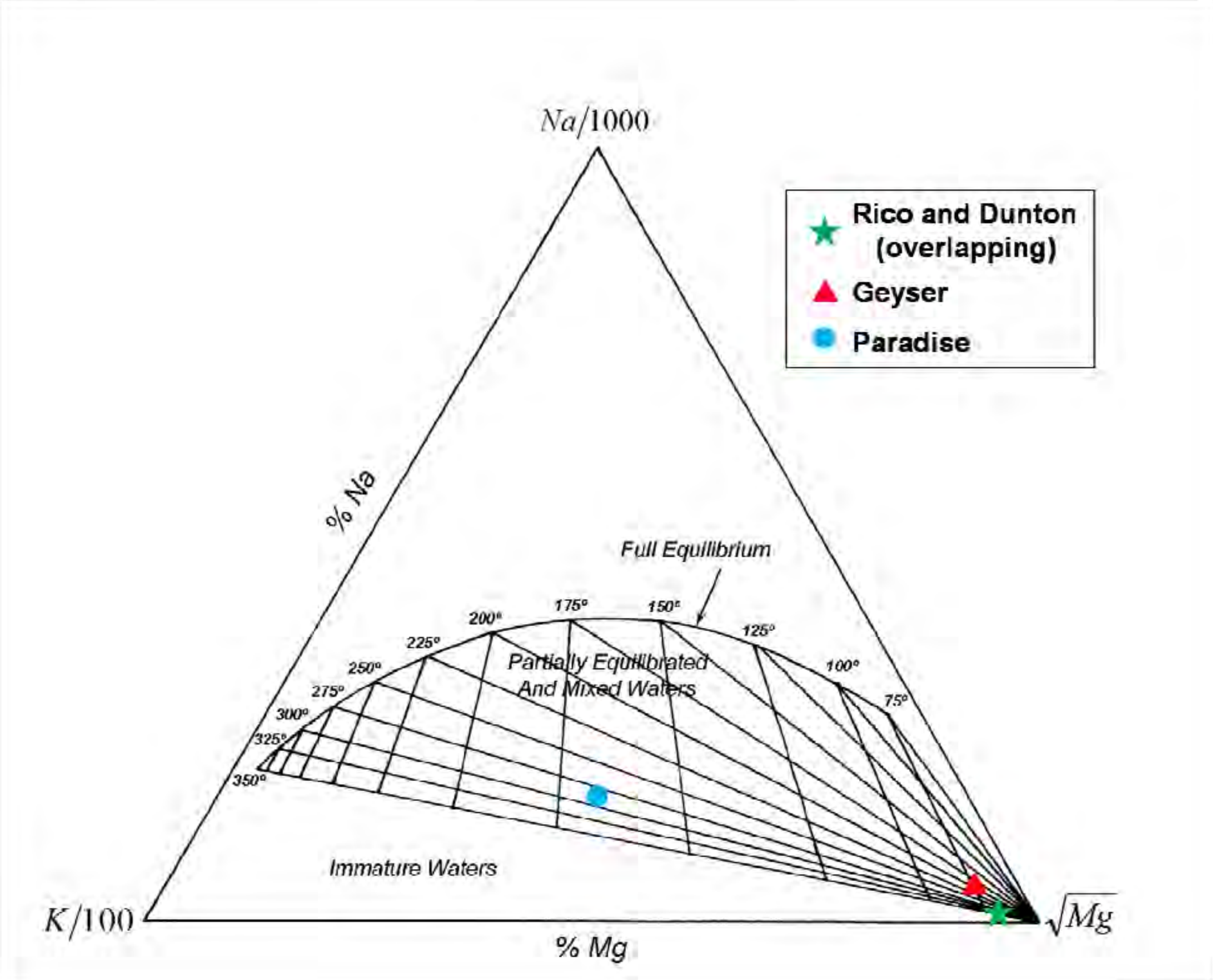

Figure 32. Giggenbach geoindicator diagram with samples plotted. The Rico and Dunton position are very similar and are plotted with one symbol for clarity.

4.7 Geothermometry Results

Geothermometer estimates of subsurface reservoir temperatures from the water samples collected in July 2008 as well as data from Barrett and Pearl, 1976, are shown in Table 7. Considering all samples, the silica geothermometers estimated temperatures between 51° C and 180° C; cation geothermometers ranged from 48° C to 155° C; and isotopic geothermometers gave estimates of 117° C to 129° C. Only geothermometers that yield reasonable results are included in these results.

The Rico Group samples all have very similar water chemistry and yield similar geothermometry estimates of subsurface temperatures. Generally, the subsurface temperature estimates yielded by the various geothermometers are either ~60° C (Na-K-Ca and K-Mg) or ~120° C to ~140° C (silica, Na-Ca, isotopes). The Rico Group is relatively close to equilibrium with both the quartz and chalcedony geothermometers with silica saturation indices of ±1 (Table 6). In contrast, the Rico Group samples are not in equilibrium with the Na-K-Mg system (Figure 32). The most likely subsurface temperature estimate for the Rico Group samples is 120° C to 140° C.

The Dunton Spring samples have similar major ion chemistry to the Rico Group samples (Tables 1 and 2), but have lower concentrations of silica which yields lower silica geothermometer estimates of ~50° C to ~90° C, although they are close to equilibrium with silica saturation (Table 6). The Na-K-Ca and K-Mg geothermometers yield estimates of ~50° C to ~65° C and the Na-Ca and isotope geothermometers yield ~115° C. The Dunton samples are not in equilibrium with the Na-K-Mg system (Figure 32). Dunton Spring subsurface temperature estimates are somewhat ambiguous, but the most likely subsurface temperature estimate is ~70°C.

Geyser Warm Spring's silica content is near equilibrium (Table 6) and yields subsurface temperature estimates of ~60° C to ~90° C (Table 7). The cation geothermometers are not in agreement with Na-K-Ca (~100° C) and K-Mg (~73° C). Isotopic geothermometers yield ~120° C. A reliable subsurface temperature estimate based on Geyser Warm Springs water chemistry is not apparent.

Paradise Spring yields the most consistent and reliable subsurface temperature estimates in this study. In terms of chemical equilibrium, Paradise water is the closest to equilibrium with silica content (2008 data, Table 6) as well as with the Na-K-Mg system (Figure 32). All of the geothermometer estimates of subsurface temperature show good agreement and indicate 120° C to 180° C.

Inclusion of the CO_2 correction to the Na-K-Ca geothermometer listed in Table 9 (Paces, 1975) does not yield reasonable estimates of subsurface temperatures for the water samples in this study and these results are not included in this discussion. No isotope geothermometer results are available for the 1970's samples because isotope analyses were not done. The Na-Ca geothermometer results for Geyser Warm Spring and Paradise Spring and the Na-K-Ca results for Paradise Spring are considered not applicable as they gave unrealistically high temperature estimates and are marked as "N/A". The Little Rico Spring sample with a potentially incorrect potassium analysis is marked with an asterisk.

Table 7. Geothermometer results summary for samples in this study (all temperatures are in ºC; NA = not applicable, NM = not measured, * indicates potential potassium data problem)

		Silica Geothermometers		Cation Geothermometers			Isotope Geothermometers	
Sample	**Measured Temperature**	**Quartz**	**Chalcedony**	**Na-K-Ca**	**K-Mg**	**Na-Ca**	**Methane – Hydrogen Gas**	**Water-Hydrogen Gas**
Rico Little Spring 9/75	38.0	131.6 - 147.8	119.7 - 122.1	15.6*	30.0*	149.4	NM	NM
Rico Little Spring 1/76	39.0	131.6 - 147.8	119.7 - 122.1	57.8	67.3	146.6	NM	NM
Rico Big Geyser 9/75	34.0	127.0 - 142.8	114.5 - 116.5	56.4	65.1	148.0	NM	NM
Rico Big Geyser 4/76	36.0	140.0 - 157.2	129.2 - 132.5	55.6	66.5	137.1	NM	NM
Rico Geyser Warm Spring 9/75	38.0	127.0 - 142.8	114.5 - 116.5	58.5	66.3	149.8	NM	NM
Rico DDH 1/76	44.0	131.6 - 147.8	119.7 - 122.1	55.5	65.6	141.3	NM	NM
Rico #1 7/2008	40.8	137.0 - 153.8	125.8 - 128.8	48.3	61.2	136.0	117.4	124.3
Rico #2 7/2008	42.8	135.3 - 151.9	123.8 - 126.6	49.6	61.1	135.3	117.3	124.3
Rico #3 7/2008	41.1	137.9 - 154.8	126.8 - 129.9	55.1	64.1	144.7	117.1	124.1
Dunton Spring 9/75	44.0	70.4 - 87.6	53.6 - 56.0	49.6	63.6	119.2	NM	NM
Dunton Spring 1/76	42.0	67.8 - 85.4	50.9 - 53.4	50.5	66.4	114.8	NM	NM
Dunton Spring 4/76	42.0	71.0 - 86.5	52.3 - 54.7	51.6	65.9	116.5	NM	NM
Dunton Spring 7/2008	41.4	75.9 - 92.3	59.3 - 61.3	47.7	62.9	113.0	117.6	124.7
Geyser Warm Spring 9/75	28.0	74.1 - 90.8	57.4 - 59.6	103.3	74.7	N/A	NM	NM
Geyser Warm Spring 7/2008	28.5	80.7 - 96.4	64.3 - 66.0	99.7	72.7	N/A	115.4	122.1
Paradise Spring 9/75	46.0	143.9 - 161.5	133.6 - 137.4	N/A	154.2	N/A	NM	NM
Paradise Spring 1/76	40.0	161.0 - 180.6	153.1 - 158.8	N/A	154.3	N/A	NM	NM
Paradise Spring 4/76	42.0	143.9 - 161.5	133.6 - 137.4	N/A	154.6	N/A	NM	NM
Paradise Spring 7/2008	43.4	150.8 - 169.2	141.5 - 146.0	N/A	154.0	N/A	121.5	129.2

5. Water and Heat Source Discussion

Geothermometry calculations can yield possible subsurface reservoir temperatures based on the chemistry of a water sample. In order to make more meaningful interpretations of these subsurface reservoir temperature estimates, it is necessary to evaluate the hydrologic and hydrochemical setting of the thermal springs.

By comparing the overall hydrochemistry of the water samples in this study, useful observations can be made. Within each spring group there is considerable spatial and temporal chemical similarity between water samples, but each group has a unique chemical composition as compared to the others. By classifying the spring waters by the dominant ionic species and plotting them into a Piper Diagram, these relationships are apparent (Figure 33). Included in this comparison figure is a Dolores River water sample that was collected by the USGS in November 1978 from the Dolores River at the nearest stream gaging station to the Rico Group, which is located just below the Town of Rico. This sample's chemical composition in terms of major ions is as follows: calcium 96 mg/L, magnesium 12 mg/L, sodium 5.6 mg/L, potassium 1.4 mg/L, bicarbonate 190 mg/L, sulfate 130 mg/L, chloride 0.9 mg/L. The composition of the West Fork Dolores River is assumed similar to the Dolores River sample.

The Rico group and the Dunton Spring samples are the most chemically similar and appear to be very similar to Dolores River water, all three being termed calcium-sulfate type waters. Geyser Warm Spring water is sodium-bicarbonate type, while Paradise Spring water is sodium-chloride type. These relationships among the major ion content of the groups is interesting because it suggests a similar source for the Rico and Dunton thermal waters, or that these springs may be composed of a large component of alluvial water. It also suggests that Paradise and Geyser Warm Spring waters are significantly different than the other waters in the study.

Similar groupings are found in the isotopic composition of the waters as shown in Figure 34. The Rico Group and Dunton Spring samples plot close together and right on or above the Local Meteoric Water Line (LMWL) which represents the ratio of deuterium to oxygen 18 atoms present in meteoric waters found in this part of the world (Figure 34). This indicates that the Rico Group and the Dunton Spring waters are very similar isotopically. Geyser Warm Spring's isotopic ratio plots lower down along the LMWL and slightly below it. Paradise Spring's isotopic composition plots higher along the LMWL than the Rico and Dunton samples and slightly below the LMWL. The small magnitude of all of the samples' shift to above or below the LMWL suggests that all of these waters are strongly dominated by meteoric water and that there may be a minor component of water that is either not meteoric in origin, or that is meteoric in origin but has undergone changes that have altered its isotopic ratio.

When considering the degree to which the surface water expression of the Rico Group and Dunton Spring is representative of the deeper thermal waters, it is important to consider the similar hydrologic setting of both the Rico Group and Dunton Spring. Situated within 200 feet of the Dolores and West Fork Dolores Rivers, and emanating from or through the alluvium in the valley bottom, it is very likely that the spring waters have mixed with shallower alluvial water as they ascended from depth. Effects of the extensive faulting present throughout the area and the possible flow paths that water has encountered are not possible to assess. It is assumed, however, that the ascending thermal waters have mixed with shallow groundwater, both diluting them chemically and cooling them down.

Paradise Spring has a similar hydrologic setting to that of the Rico Group and Dunton Spring, however the water is a sodium-chloride type and is unique among water samples in this study with very high specific conductance (~10 mS/cm) and elevated concentrations of lithium (~9 mg/L), potassium (~370 mg/L), sodium (~1900 mg/L) and chloride (~3100 mg/L) (Figure 33, Table 2). Paradise Spring water is also distinct isotopically, plotting higher along the LMWL than other samples in this study, although it is still very close to the LMWL (Figure 34). The extent to which Paradise Spring water is mixed with shallow groundwater or alluvial water is uncertain given its distinct chemical composition juxtaposed with is location directly adjacent to the West Fork Dolores River in the valley bottom alluvium.

Geyser Warm Spring is unique in this study, as it is not situated in a river valley bottom and the surface temperature of its water is lower than the other springs (~28° C vs. ~40° C). Chemically and isotopically, the water is distinct as well (Figures 33 and 34). Geyser Warm Spring is situated in a steep-sided, rocky canyon approximately 30 feet above a small stream that flows in a bedrock channel, and ~600 feet in elevation above the West Fork Dolores river valley. Geyser Warm Spring waters are likely mixed with shallow groundwater that exists in fractures in the bedrock. The low surface temperature of Geyser Warm Spring may be explained by a high degree of mixing with shallow groundwater coupled with increased residence time in bedrock fractures as the waters migrate to the surface.

While the individual springs each have a specific chemical signature indicating a unique geochemical evolution, it is likely that all of the springs' waters are meteoric in origin, given their similar isotopic composition to local meteoric waters (Figure 34). It is also likely because of the springs close geographic proximity to each other, that the meteoric waters that are circulating in both the alluvial and deeper aquifers in the area are heated by the same subsurface heat source.

Temperature data from mineral exploration drill holes within a 3.5 km radius of the Town of Rico yield geothermal gradients ranging from 24 to 114°C km^{-1} (Medlin, 1983; Decker et al., 1988; unpublished mining data, compiled 2009, personal communication M. Nakagawa, 2010). Therefore, meteoric water circulation depths ranging from about 0.5 to >2.5 km are necessary to meet the range of subsurface reservoir temperatures predicted by the geothermometers. Temperature data from two drill holes within a 0.75 km radius of the geochemical sampling points north of Rico yield geothermal gradients of 91 and 92°C km^{-1}, narrowing down the probable range of meteoric water circulation depths to 0.6 to 1.9 km.

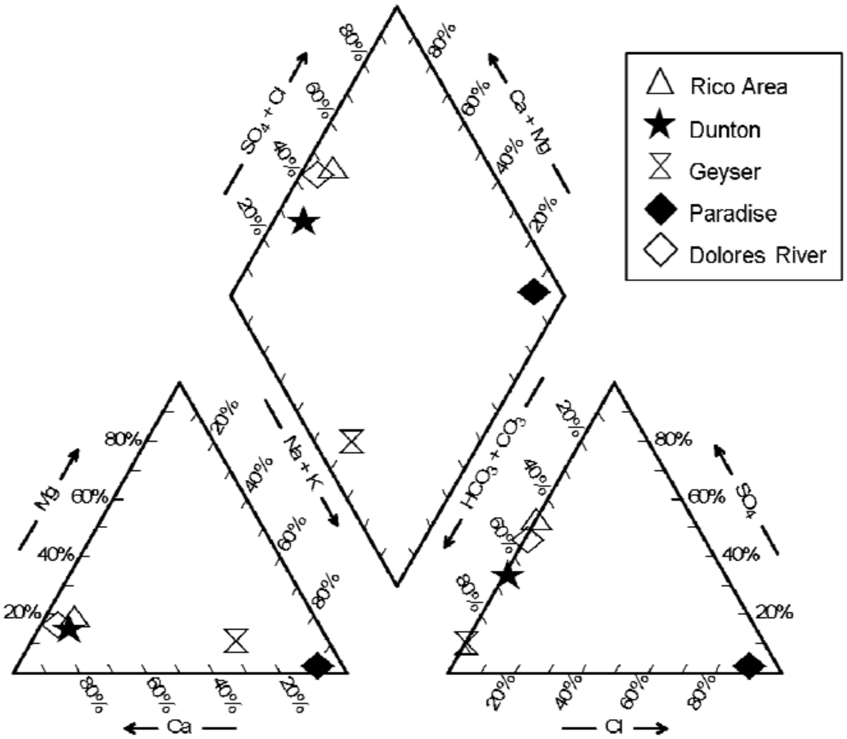

Figure 33. Piper Diagram for water samples from the spring groups in this study. For clarity, one symbol is plotted for each spring group which represents the general plotted vicinity of all of the samples of that group. Note the plotted location of a sample of Dolores River water, taken from below the Town of Rico in 1978.

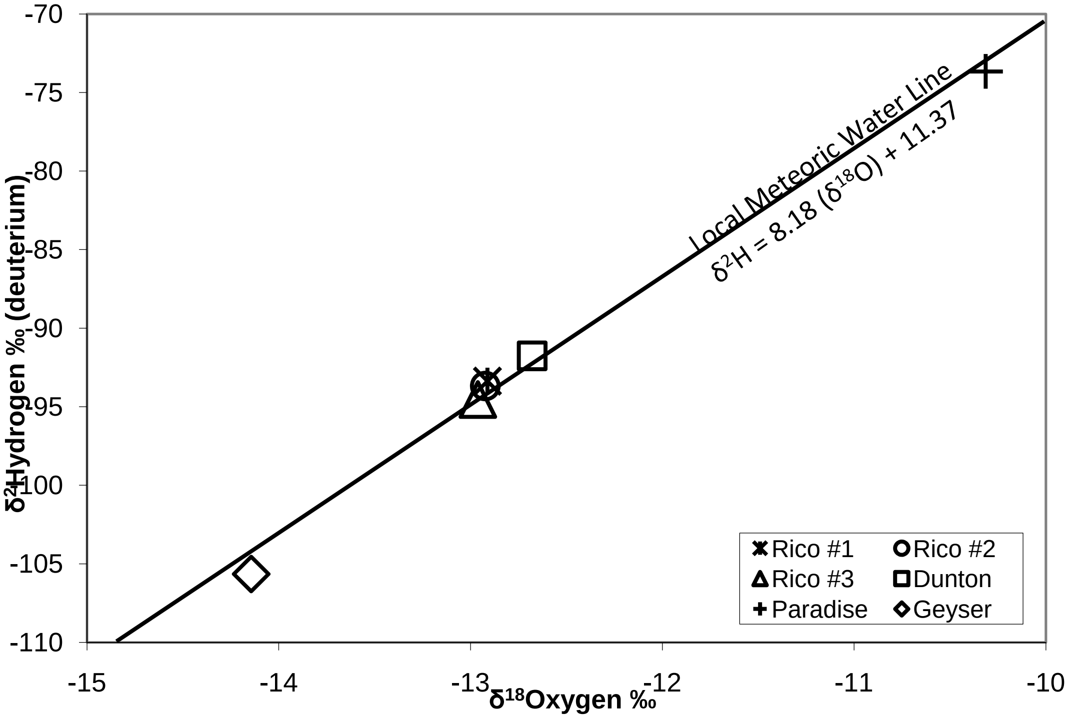

Figure 34. Plot of the ^{2}H and ^{18}O isotopic composition of 2008 water samples

6. Conclusions

This study was undertaken to determine whether advances in the science and practice of geothermometry could allow for better control and confidence in the estimation of the temperature of the geothermal resource at depth in the Rico, Dunton, and West Fork Dolores River areas. In broad terms, the warm spring waters examined in this study remain ambiguous with respect to a definitive subsurface temperature estimate. The geothermal systems represented by the water samples examined in this study are extremely complex. The factors affecting the chemistry of these waters include complex regional geologic structure and mineralization, difficult to assess hydrogeology, and the anthropogenic effects of mining and mineral exploration overprinting the natural system.

All geothermometry models are based on various assumptions, that when satisfied, allow for some level of confidence in the subsurface temperature estimates generated. In the case of the waters examined in this study, nearly all of these assumptions have the potential to be unsatisfied. Nevertheless, geothermometer estimates of subsurface temperature can be combined with chemical, isotopic, and hydrologic analyses and can give insight into the qualities of the subsurface heat source in the area.

Geothermometer calculations applied to these data, and to previous 1970's water chemistry data, variously estimate subsurface reservoir temperatures ranging from 60°C to 150°C. Springs in the West Fork Dolores River valley have relative agreement between silica and K-Mg geothermometers, with subsurface temperatures at Dunton and Geyser Warm Springs of ~60-70°C, and at Paradise Spring of ~150°C. Samples from the Rico area springs exhibit less agreement, with silica geothermometers giving subsurface temperature estimates of ~120-150°C, whereas K-Mg and Na-K-Ca geothermometers estimate ~60°C.

7. Acknowledgements

This study was jointly funded by the State of Colorado Governor's Energy Office and the Colorado Geological Survey (Colorado Department of Natural Resources Severance Tax Operational Fund). This report benefitted greatly from helpful and insightful reviews by M. Sares, P. Morgan, J. Moore, and M. Ausburn.

8. References

Arnórsson, Stefán; Gunnlaugsson, Einar; Svavarsson, Hördur; 1983, The chemistry of geothermal waters in Iceland. III. Chemical geothermometry in geothermal investigations: Geochimica Cosmochimica Acta, v. 47, p. 567-577.

Arnórsson, Stefán; Andresdottir, Agústa; Gunnarsson, Ingvi; Stefánsson, Andri; 1998, New calibration for the quartz and Na/K geothermometers – valid in the range 0-350ºC, *in* Proceedings of the Geoscience Society of Iceland Annual Meeting, April 1994, p. 42 – 43.

Barrett, J.K., and Pearl, R.H., 1976, Hydrogeological data of thermal springs and wells in Colorado: Information Series 6: Denver, CO, Colorado Geological Survey, 124 p.

Barrett, J.K., and Pearl, R.H., 1978, An appraisal of Colorado's geothermal resources: Bulletin 39: Denver, CO, Colorado Geological Survey, 224 p.

Berkman, Frederick J., and Carroll, Christopher J., 2007, Interpretive geothermal heat flow map of Colorado: Colorado Geological Survey Map Series 45, 2 Plates.

Berkman, Frederick J., and Watterson, Nicholas, 2010, Interpretive geothermal gradient map of Colorado: Colorado Geological Survey Map Series 46, 3 plates.

Bottinga, Yan, 1969, Calculated fractionation factors for carbon and hydrogen isotope exchange in the system calcite-carbon dioxide-graphite-methane-hydrogen-water vapor: Geochimica Cosmochimica Acta, v. 33, p. 49-64.

Bush, A.L. and Bromfield, C.S., 1966, Geologic map of the Dolores Peak quadrangle, Dolores and San Miguel counties, Colorado: United States Geological Survey, GQ-536, 1 plate.

Cappa, J.A., and Hemborg, H.T., 1995, Low temperature geothermal assessment program 1992-1993: Colorado Geological Survey Open-File Report 95-1, 20 pages, 1 plate.

D’Amore, Franco; and Arnórsson, Stefán; 2000, Geothermometry, *in* Isotopic and chemical techniques in geothermal exploration, development and use, ed. S. Arnórsson, International Atomic Energy Agency, Vienna, p.152-199.

Decker, E.R., Heasler, H.P., Buelow, K.L., Baker, K.H., and Hallin, J.S., 1988, Significance of past and recent heat-flow and radioactivity studies in the southern Rocky Mountains region: Geological Society of America Bulletin, v. 100, no. 12, p. 1851-1885.

Fournier, R.O., 1977, Chemical geothermometers and mixing models for geothermal systems: Geothermics, v. 5, p. 41-50.

Fournier, R.O., 1979, A revised equation for the Na/K geothermometer, Geothermal Resources Council Transactions, v. 3, p. 221-224.

Fournier, R.O. and Potter, R.W. II, 1979, Magnesium correction to the Na-K-Ca geothermometer: Geochimica Cosmochimica Acta, v. 343, p. 1543-1550.

Fournier, R.O. and Potter, R.W. II, 1982, A revised and expanded silica (quartz) geothermometer: Geothermal Resource Council Bulletin, V. 11, p. 3-9.

Fournier, R.O., and Truesdell, A.H., 1973, An empirical Na-K-Ca geothermometer for natural waters: Geochimica Cosmochimica Acta, v. 37, p. 155-1275.

Fournier, R.O., White, D.E., and Truesdell, A.H., 1974, Geochemical indicators of subsurface temperature - 1. Basic assumptions.: United States Geological Survey Journal of Research, v. 2, p. 259-262.

Giggenbach, W.F., 1988, Geothermal solute equilibria: Geochimica Cosmochimica Acta, v. 52, p. 2749-2765.

Kharaka, Y.K., Lico, M.S., Law, L.M., 1982, Chemical geothermometers applied to formation waters, Gulf of Mexico and California Basins: American Association of Geologists Bulletin, v. 66, p. 538.

Kharaka, Y.K. and Mariner, R.H., 1988, Chemical geothermometers and their application to formation of waters from sedimentary basins, *in* Thermal History of Sedimentary Basins, *eds* Naser, N.D., McCollin, T.H., Springer-Verlag, New York, p. 99-117.

Lloyd, R.M., 1968, Oxygen isotope behaviour in the sulfate-water system: Journal of Geophysical Research, v. 73, p. 6099.

Medlin, E. W., 1983, Modeling Local Thermal Anomalies: Constraints from Conductivity, Gravity and Heat Flow, M.S. Thesis, Dept. Geology & Geophysics, Univ. Wyoming, Laramie, Wyoming.

Mizutani, Y. and Rafter, T.A., 1969, Oxygen isotope composition of sulphates. Oxygen isotope fractionation in the bisulphate ion-water system: New Zealand Journal of Science, v. 12, p. 54.

Nieva, D., and Nieva, R., 1987, Developments in geothermal energy in Mexico, Part 12. A cationic geothermometer for prospecting of geothermal resources: Heat Recovery Systems & CHP, v. 7, p. 243-258.

Paces, Tomas; 1975, A systematic deviation from the Na-K-Ca geothermometer below 75ºC and above 10^{-4} atm. P_{CO2}: Geochimica Cosmochimica Acta, v. 39, p. 541-544.

Parkhurst, D.L. and Appelo, C.A.J., 1999, User’s guide to PHREEQC (Version 2)—A computer program for speciation, batch-reaction, one-dimensional transport, and inverse geochemical calculations: United States Geological Survey Water-Resources Investigations Report 99-4259, 310 p.

Pratt, W.P., McKnight, E.T., DeHon, R.A., 1969, Geologic map of the Rico quadrangle, Dolores and Montezuma counties, Colorado: United States Geological Survey, GQ-797, 1 plate.

Richet, Pascal; Bottinga, Yan; Javoy, Marc; 1977, A review of hydrogen, carbon, nitrogen, oxygen, sulfur and chlorine stable isotope fractionation among gaseous molecules: Ann. Reg. Earth Planet. Sci., v. 5, p. 65-110.

Tonani, Franco; 1980, Some remarks on the application of geochemical techniques in geothermal exploration: Proc. Adv. Eur. Geoth. Res., 2nd Symp., Strasbourg, p. 428-443.

Truesdell, A.H., 1976, Summary of Section III. Geochemical techniques in exploration: Second United Nations Symposium on the Development and Use of Geothermal Resources, San Francisco, p. 53-79.

9. Appendices

9.1 Appendix A – Sampling Methods

Initial Sampling Methods

1) Record all observations and measurements on a Water Sample Data Sheet: Perform requisite measurements of geographic location with the use of a Magellan Meridian Platinum handheld GPS device, physical description, weather and other comments. Perform temperature measurements as close to the actual upwelling source of the spring in the spring pool as possible. When performing temperature measurements, take 3 to 5 readings and then average these readings. Temperature measurements were made with both an Oakton pH/conductivity/temperature meter (model number 35630-02) as well as a digital probe-type thermometer to corroborate the Oakton meter readings. Volumetric discharge measurements of the springs were not possible due to the spring pool usually being located atop a precipitate mound with water discharging in a radial fashion out of the spring pool and over the surface of the precipitate mound.

2) Collect Bulk Samples (two 1000-mL bulk samples). Label two 1000-mL HDPE bottles with the spring name and give each bulk sample bottle a unique identifier, e.g. Paradise Warm Spring #1 etc. Rinse each clean, unused 1000-mL sample bottle with the sample water *three times*. Then fill it with sample water. *Do not touch the inside of the bottle, the lid, or the sample water.*

3) Transport the bulk samples to the sub-sampling location and begin the sub-sampling procedure as quickly as possible.

At the sub-sampling location:

4) Assemble the sub-sampling cooling and filtering apparatus as follows (listed from upstream to downstream in the sampling flow, bulk sample to sub-samples): a ~3-ft length of flexible tubing with a 0.25 inch inside diameter, a cooling coil made from 0.25 inch outside diameter T-316 stainless steel tubing (~16 ft in length, coiled into ~5 inch diameter coils), a ~5-ft length of 0.25 inch inside diameter flexible tubing that is compatible with sampling pump being used (Cole-Parmer Instrument Company Masterflex E/S Portable Sampling Pump), adapter tubing to allow connection of 0.45 micron filter being used (Geotech Environmental Equipment #75050004), a short length (~ 2 ft) of extension tubing compatible with outflow side of filter to dispense sample into sub-sample bottles (Figures 4 and 5). Place cooling coil into 5-gallon bucket filled with ice and/or cold water. Place flexible tubing downstream of cooling coil into sampling pump jaws, close pump jaws onto tubing.

5) Flush sampling system with deionized or distilled water so that contaminants and previous waters are expelled from the system. Adjust the pump speed so that the water coming out of the downstream end of the system is as cold as possible. This is typically the minimum pump speed that will still allow enough volume flow through the system. Release pump jaws so that the flush water within the system can be expelled using pneumatic pressure or by gravity drain.

6) Label two 250-mL HDPE and one 60-mL glass bottle with poly seal cap according to the following scheme:

> RICO-08-01-A (Project – Year – Sample # - Subsample type) for the acidified, filtered sample which will be used for dissolved metals analysis (250 mL).
> RICO-08-01-B for the unfiltered, unacidified sample which will be analyzed for various constituents (250 mL).
> RICO -08-01-C for the filtered, unacidifed sample which will be analysed for ^{2}H and ^{18}O stable isotopes (60 mL).
>
> Record such details as date, sample type, sampler, etc.

7) Acidify the “A” sample bottle with 20 drops of concentrated, reagent grade HNO_3 (nitric acid).

8) Begin sub-sampling by pumping water from the bulk sample bottle through the cooling coil, through the pump, through the filter, and into bottles “A” and “C”. Fill these bottles as full as possible in order to minimize or eliminate headspace. Shut down pump and place outlet tubing of system in a secure manner that will not contaminate it. Cap bottles “A” and “C”.

9) Remove filter and extension tubing from system. Begin pumping unfiltered sample water into bottle “B,” again filling bottle so that there is little to no headspace. Shut down pump and cap “B” bottle.

10) Immediately place all three bottles into plastic bags and place in a cooler with ice or reusable cooler packs to keep samples cool.

11) Flush sampling system with deionized or distilled water to remove any sample water from system. Release pump jaws and expel water from system with pneumatic pressure or gravity drain.

12) Perform pH, conductivity, dissolved oxygen and alkalinity measurements on remaining bulk sample water. There should be approximately 1 liter of bulk sample water left after sub-sampling. Note: If possible, perform these measurements while at the sampling site. If not possible, perform these measurements as soon as possible after the initial collection of the bulk sample.

> 12a) Calibrate the pH meter according to manufacturer’s instructions and perform pH measurements on the bulk sample.
>
> 12b) Calibrate the conductivity meter according to the manufacturer’s instructions and perform conductivity measurements on the bulk sample.
>
> 12c) Calibrate the dissolved oxygen meter according to the manufacturer’s instructions and perform dissolved oxygen tests.
>
> 12d) Conduct an alkalinity test using Chemetrics K-9820 alkalinity test vials according to manufacturer’s instructions.

13) Package samples into coolers with ice or reusable cooler packs for shipping to laboratory.

14) Ship coolers with samples to laboratory for analysis. Adhere to guidelines regarding specific holding times for certain types of analyses (typically 48 hours for various ions in solution).

9.2 Appendix B – Available Geothermometer Equations

Table 8. Available silica geothermometer equations (after D’Amore and Arnorsson, 2000).

Temperature Equations for the Silica Geothermometers
(S represents silica concentration as SiO_2 in mg/kg,
with concentrations of silica found in these waters mg/kg = mg/L = ppm)

Equation #	Geothermometer	Equation (T in ºC)	Range (ºC)	Source
1	Quartz	$\frac{1309}{5.19-\log S}-273.15$	25-250	Fournier (1977)
2	Quartz	$\frac{1522}{5.75-\log S}-273.15$	25-250	Fournier (1977)
3	Quartz	$-42.2+0.28831S-3.6686\times10^{-4}S^{2}$ $+3.1665\times10^{-7}S^{3}+77.034\log S$	25-900	Fournier and Potter (1982)
4	Quartz	$-53.5+0.11236S-0.5559\times10^{-4}S^{2}$ $+0.1772\times10^{-7}S^{3}+88.390\log S$	Not Reported	Fournier and Potter (1982)
5	Quartz	$-55.3+0.3659S-5.3954\times10^{-4}S^{2}$ $+5.5132\times10^{-7}S^{3}+74.360\log S$	0-350	Arnorsson et al. (1998)
6	Quartz	$-66.9+0.1378S-4.9727\times10^{-5}S^{2}$ $+1.0468\times10^{-8}S^{3}+87.841\log S$	0-350	Arnorsson et al. (1998)
7	Chalcedony	$\frac{1032}{4.69-\log S}-273.15$	0-250	Fournier (1977)
8	Chalcedony	$\frac{1112}{4.91-\log S}-273.15$	Not Reported	Arnorsson et al. (1983)
9	Amorphous Silica	$\frac{731}{4.52-\log S}-273.15$	25-250	Fournier (1977)
10	Amorphous Silica	$-121.6+0.2694S-1.8101\times10^{-4}S^{2}$ $+7.5221\times10^{-8}S^{3}+55.114\log S$	0-350	D’Amore and Arnorsson (2000)

Table 9. Available cation geothermometer equations (after D'Amore and Arnorsson, 2000).

Temperature Equations for Cation Geothermometers
(Concentrations are in ppm if not otherwise specified,
with concentrations of cations found in this study ppm = mg/L = mg/kg)

Equation #	Geothermometer	Equation (T in ºC)	Range (ºC)	Source
1	Na-K	$\frac{856}{0.857+\log(Na/K)}-273.15$	100-275	Truesdell (1976)
2	Na-K	$\frac{1217}{1.438+\log(Na/K)}-273.15$	Not Reported	Fournier (1979)
3	Na-K	$\frac{833}{0.780+\log(Na/K)}-273.15$	Not Reported	Tonani (1980)
4	Na-K	$\frac{933}{0.993+\log(Na/K)}-273.15$	25-250	Arnorsson et al. (1983)
5	Na-K	$\frac{1319}{1.669+\log(Na/K)}-273.15$	250-350	Arnorsson et al. (1983)
6	Na-K	$\frac{1178}{1.470+\log(Na/K)}-273.15$	Not Reported	Nieva and Nieva (1987)
7	Na-K	$\frac{1390}{1.750-\log(Na/K)}-273.15$	Not Reported	Giggenbach (1988)
8	Na-K	$733.6-770.551Y+378.189Y^2-95.753Y^3+9.544Y^4$	0-350	Arnorsson et al. (1998)
9	K-Mg	$\frac{4410}{14.0-\log(K^2/Mg)}-273.15$	< 100	Giggenbach (1988)
10	Li-Mg	$\frac{2200}{5.470-\log(Li/Mg^{0.5})}-273.15$	Not Reported	Kharaka and Mariner (1988)
11	Na-Li	$\frac{1590}{0.779+\log(Na/Li)}-273.15$	Not Reported	Kharaka et al. (1982)
12	Na-Ca	$\frac{1096.7}{3.08+\log(Na/Ca^{0.5})}-273.15$	Not Reported	Tonani (1980)
13	Na-K-Ca [Conc] in mol/kg B=4/3 for T<100ºC B=1/3 for T>100º and $\log(Ca^{0.5}/Na)<0$	$\frac{1647}{\log(Na/K)+\beta\log(Ca^{0.5}/Na)+2.24}-273.15$	Not Reported	Fournier and Truesdell (1973)
13.1	CO_2 Correction to Na-K-Ca	"2.24" term in Na-K-Ca is replaced with "I" $I=-1.36-0.253\log P_{CO_2}$ $\log P_{CO_2}=-3.78+0.0168T$ With T = measured temperature (°C)	Not Reported	Paces (1975)

Table 10. Available isotopic geothermometer equations (after D'Amore and Arnorsson, 2000).

Temperature Equations for Isotopic Geothermometers
(with α=δ (Isotope) in ‰ VSMOW)

Equation #	Reaction	Equation (T_K in Kelvin)	Source
1	$CH_3D + H_2 = HD + CH_4$ (methane - hydrogen gas)	$1000 \ln\alpha = 288.9\times10^3/T_K + 31.86\times10^6/T_K{}^2 - 238.28$ Valid in range 100 - 400° C	Bottinga (1969) Richet et al (1977)
2	$HD + H_2O = H_2 + HDO$ (water - hydrogen gas)	$1000 \ln\alpha = 396.8\times10^3/T_K + 25.196\times10^6/T_K{}^2 - 284$ Valid in range 100 - 400° C	Richet et al (1977)
3	$S^{16}O_4 + H_2{}^{18}O = S^{16}O_3{}^{18}O + H_2{}^{16}O$ (sulfate - water)	$1000 \ln\alpha = 3.25\times10^6/T_K{}^2 - 5.6$ Valid in range 100 - 350° C	Lloyd (1968)
4	$S^{16}O_4 + H_2{}^{18}O = S^{16}O_3{}^{18}O + H_2{}^{16}O$ (sulfate - water)	$1000 \ln\alpha = 2.88\times10^6/T_K{}^2 - 4.1$ Valid in range 100 - 350° C	Mizutani and Rafter (1969)
5	$C^{16}O_2 + H_2{}^{18}O = C^{16}O^{18}O + H_2{}^{16}O$ (carbon dioxide - water)	$1000 \ln\alpha = -18.29\times10^3/T_K + 7.626\times10^6/T_K{}^2 - 19.6$ Valid in range 100 - 400° C	Richet et al (1977)